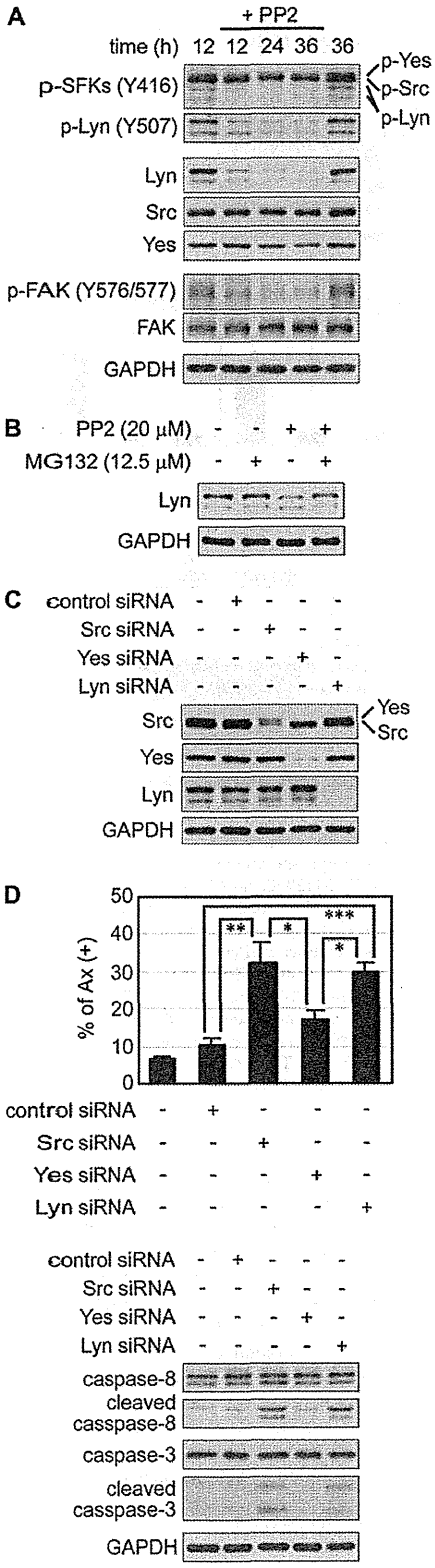

Fig. 4. Src and Lyn suppress apoptosis accompanied by caspase-8 activation in Fyn-deficient mesothelioma cells. (**A**) PP2 inhibits SFK activity and reduces Lyn protein levels. Cell extracts were prepared from NCI-H28 cells treated with 20 μM PP2 for 12–36 h. (**B**) Lyn protein is degraded by the ubiquitin-proteasome pathway. Cell extracts were prepared from NCI-H28 cells treated with 20 μM PP2 together with 12.5 μM MG132 for 12 h. (**C**) Knockdown of Src, Yes and Lyn in NCI-H28 cells. The cells were transfected with Src, Yes and Lyn siRNAs and control siRNA for 48 h, harvested by trypsinization and incubated for 24 h, and cell extracts were prepared as described in Materials and methods. (**D**) Src and Lyn siRNAs, but not Yes siRNA, significantly induce apoptosis accompanied by caspase-8 activation in NCI-H28 cells. The cells were transfected with Src, Yes and Lyn siRNAs and control siRNA for 48 h, harvested by trypsinization and incubated for 24 h. The old medium was exchanged after the incubation for 24 h, and the cells were incubated further for 72 h and analyzed for Ax (+) apoptotic cells by flow cytometry. For western blotting, cell extracts were prepared from NCI-H28 cells incubated for 72 h after the medium exchange.

Tyr-507 in Lyn (Figure 4A). PP2 also induced reduction of Lyn protein levels but not Src or Yes protein levels. These results suggest that PP2-inhibited Lyn phosphorylation is caused by reduction of Lyn protein. Lyn protein has been reported to be degraded by the ubiquitin-proteasome pathway (14). Therefore, we examined the involvement of this pathway. MG132, a proteasome inhibitor, suppressed PP2-induced reduction of Lyn protein (Figure 4B), suggesting that Lyn protein is degraded by the ubiquitin-proteasome pathway. To investigate which SFKs are involved in apoptosis mediated by caspase-8 in Fyn-deficient mesothelioma cells, we analyzed the induction of apoptosis in NCI-H28 cells treated with siRNAs targeting Src, Yes and Lyn. Each siRNA abrogated expression of respective SFK protein (Figure 4C). Src and Lyn siRNAs, but not Yes siRNA, significantly induced apoptosis in NCI-H28 cells (Figure 4D). In addition, knockdown of Src and Lyn, but not of Yes, induced cleavage of caspase-8 and caspase-3. These results suggest that Src and Lyn suppress caspase-8 activation and apoptosis in Fyn-deficient mesothelioma cells.

Both Fyn and Lyn suppress apoptosis in mesothelioma cells

We analyzed whether Src, Yes and Lyn are involved in apoptosis in Fyn-expressing mesothelioma cells (Figure 5). In NCI-H2052 and ACC-MESO-4 cells treated with Fyn siRNA and control siRNA, PP2 suppressed FAK phosphorylation and reduced Lyn protein levels (Figure 5A), whereas PP2 failed to induce caspase-8 cleavage and apoptosis in these cells treated with control siRNA (Figure 3B and C). We then investigated apoptotic induction by RNAi knockdown of Src, Yes and Lyn in Fyn-expressing mesothelioma cells. Individual siRNAs abrogated expression of respective SFK protein but failed to induce apoptosis in NCI-H2052 and ACC-MESO-4 cells (Figure 5B). We further performed knockdown of both Fyn and Lyn. The double knockdown of Fyn and Lyn efficiently abrogated expression of both Fyn and Lyn with no effect on expression of Src and Yes protein (Figure 5C). The double knockdown induced significant apoptosis and cleavage of caspase-8 and caspase-3 in NCI-H2052 and ACC-MESO-4 cells (Figure 5D). Collectively, these results show that PP2-induced apoptosis is caused by reduction of Lyn protein in Fyn-deficient mesothelioma cells.

SFK inhibitors induce reduction of Lyn protein followed by caspase-8-dependent apoptosis in Fyn-deficient mesothelioma cells

To further investigate whether other SFK inhibitors are able to induce apoptosis in Fyn-deficient mesothelioma cells, we treated these cell lines with dasatinib, an inhibitor of multi-tyrosine kinase including Bcr-Abl kinase and SFK (Figure 6). Dasatinib suppressed cell viability of all MM cell lines used more markedly than that of Met5A cells in a concentration-dependent manner (Figure 6A). In addtion, Dasatinib significantly induced apoptosis in NCI-H28 cells but not other mesothelioma cell lines (Figure 6B). Dasatinib inhibited phosphorylation of SFKs and FAK, reduced Lyn protein, but not of Src and Yes protein levels and cleavage of caspase-8 and caspase-3 in a concentration- and time-dependent manner in NCI-H28 cells (Figure 6C). Dasatinib also induced reduction of Lyn protein levels in NCI-H2052 and ACC-MESO-4 cells (data not shown) but failed to induce cell death in these Fyn-expressing mesothelioma cell lines

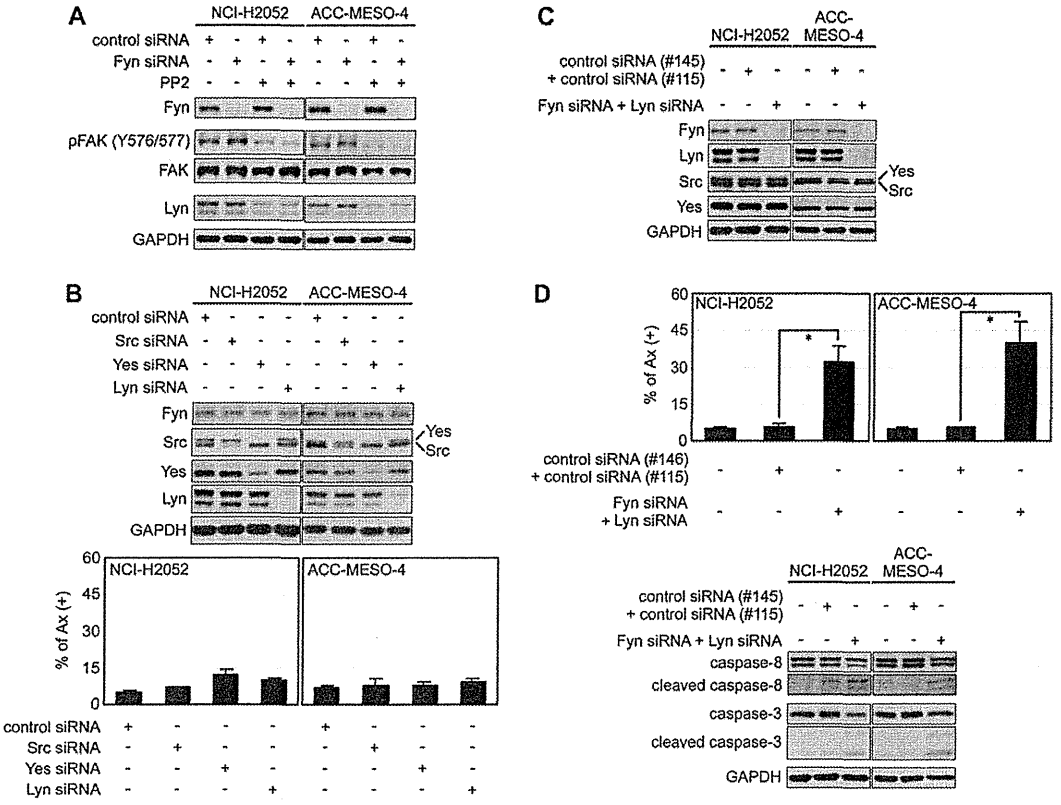

Fig. 5. Both Fyn and Lyn suppress apoptosis accompanied by caspase-8 activation in mesothelioma cells. (**A**) PP2 inhibits SFK activity and reduces Lyn protein levels without Fyn-knockdown in mesothelioma cells. NCI-H2052 and ACC-MESO-4 cells, transfected with Fyn and control siRNAs, were treated with 20 μM PP2 for 24 h. (**B**) siRNA of individual SFK fails to induce apoptosis in Fyn-expressing mesothelioma cells. NCI-H2052 and ACC-MESO-4 cells were transfected with Src, Yes and Lyn siRNAs and control siRNA for 48 h, harvested by trypsinization and further incubated at 37°C for 24 h. For western blotting, cell extracts were prepared from NCI-H2052 and ACC-MESO-4 cells after the incubation for 24 h. The old medium was exchanged after the incubation for 24 h, and the cells were incubated further for 72 h and analyzed for Ax (+) apoptotic cells by flow cytometry. (**C**) Double knockdown of Fyn and Lyn in Fyn-expressing mesothelioma cells. NCI-H2052 and ACC-MESO-4 cells were transfected with both Fyn and Lyn siRNAs or both control siRNA (#146) and control siRNA (#115) for 48 h. The cells were harvested by trypsinization and incubated for 24 h. Cell extracts were prepared from NCI-H2052 and ACC-MESO-4 cells after the incubation for 24 h. (**D**) Double knockdown of Fyn and Lyn induces apoptosis accompanied by caspase-8 activation in mesothelioma cells. NCI-H2052 and ACC-MESO-4 cells were transfected with both Fyn and Lyn siRNAs or both control siRNA (#146) and control siRNA (#115) for 48 h, and the cells were harvested by trypsinization and further incubated at 37°C for 24 h. The old medium was exchanged after the incubation for 24 h. The cells were incubated further for 72 h and analyzed for Ax (+) apoptotic cells by flow cytometry. For western blotting, cell extracts were prepared from NCI-H2052 and ACC-MESO-4 cells incubated for 72 h after the medium exchange.

(Figure 6B). These results suggest that dasatinib, like PP2, is able to induce caspase-8-dependent apoptosis mediated by reduction of Lyn protein in Fyn-deficient mesothelioma cells.

Discussion

Malignant mesothelioma is refractory to conventional chemotherapy, which is related to the resistance to induction of apoptosis by chemotherapeutic agents (3). PP2 has been shown to induce apoptosis in some tumor cells, including B-cell leukemia and breast cancer and hepatoma but not in primary hepatocytes (15–17). In the present study, we found that PP2 induced apoptosis mediated by caspase-8 in a mesothelioma cell line, NCI-H28, but not a non-malignant mesothelioal cell line, Met5A (Figure 1).

Fyn is generally expressed in various tissues (7). Fyn has been recognized as an important mediator of cell cycle, growth, survival and cell–cell adhesion (18). Western blot and quantitative reverse transcription–PCR analyses revealed that Fyn protein is detected in all cell lines used except NCI-H28 cells, and Fyn synthesis is suppressed by transcriptional repression of Fyn mRNA in NCI-H28 cells (Figure 2). In prostate cancer, Fyn is reported to be downregulated by both chromosomal deletion and promoter hypermethylation (19). However, Fyn promoter regions were not methylated in NCI-H28 cells (data not shown). Detailed investigation to clarify how transcription of Fyn mRNA is repressed in NCI-H28 cells is needed. We also found that Fyn-knockdown facilitated PP2-induced apoptosis in mesothelioma cells (Figure 3). Furthermore, we observed that Fyn-expressing mesothelioma cells were resistant to apoptosis induced by SFK inhibition and knockdown of individual SFK (Figures 3 and 5). Fyn is overexpressed in various cancers, including glioblastoma, squamous cell carcinoma, melamona and chronic myeloid leukemia (18,20). In addition, chronic myeloid leukemia cells overexpressing Fyn have been shown to be resistant to PD166326, a Bcr-Abl kinase and SFK inhibitor (21). We found that Fyn-knockdown or deficiency of Fyn protein is insufficient to induce apoptosis but facilitated PP2-induced apoptosis in mesothelioma cells (Figures 1–3).

Lyn is known to be expressed in all blood cells except T lymphocytes (22). In neutrophils, PP2 is reported to reduce Lyn protein levels and apoptosis accompanied by caspase-8 activation (12). Our results revealed that Lyn is expressed in mesothelial and mesothelioma cells and degraded by the ubiquitin-proteasome pathway in mesothelioma cells (Figures 2 and 4). In addition, Lyn-knockdown induced apoptosis accompanied by caspase-8 activation in NCI-H28 cells (Figure 4). However, PP2-induced reduction of Lyn protein levels

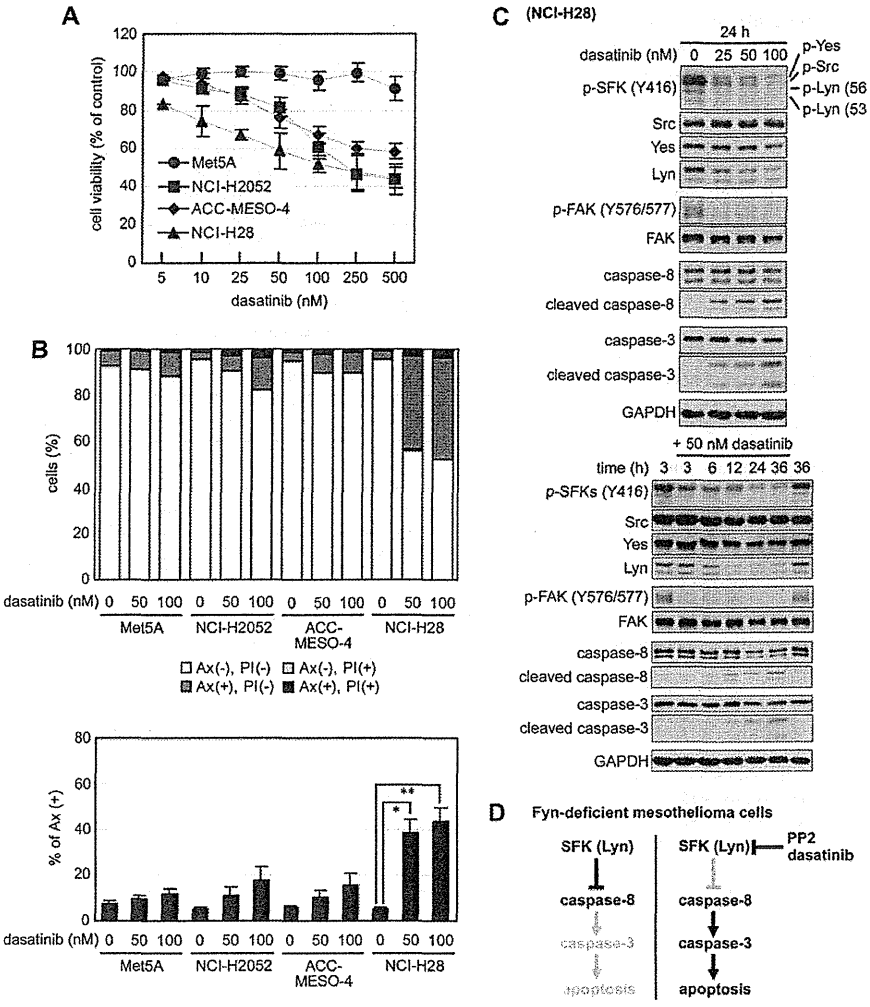

Fig. 6. SFK inhibitors induce reduction of Lyn protein followed by caspase-8-dependent apoptosis in Fyn-deficient mesothelioma cells. (**A**) Dasatinib suppresses cell viability of NCI-H2052, ACC-MESO-4 and NCI-H28 cells more markedly than that of Met5A cells. These cell lines were treated with dasatinib for 48 h at the indicated concentrations. Cell viability was assessed using the Cell Counting Kit-8 assay. (**B**) Dasatinib induces apoptosis in NCI-H28 cells more significantly than that in Met5A cells. Met5A, NCI-H2052, ACC-MESO-4 and NCI-H28 cells were treated with 50 and 100 nM dasatinib for 72 h and analyzed for Ax (+) apoptotic and propidium iodide (PI) (+) positive cells by flow cytometry. (**C**) Dasatinib inhibits SFK activity and reduces Lyn protein levels and caspase-8 activation in NCI-H28 cells. Cell extracts were prepared from NCI-H28 cells treated with dasatinib for 3–36 h at the indicated concentrations. (**D**) Schematic mechanism of apoptosis induced by SFK inhibitors in Fyn expression-suppressed mesothelioma cells. In Fyn expression-suppressed mesothelioma cells, SFK, in particular Lyn, suppresses caspase-8 activation (left panel), whereas SFK inhibitors, PP2 and dasatinib, reduce Lyn protein and apoptosis mediated by caspase-8 (right panel).

and Lyn-knockdown failed to induce apoptosis in other mesothelioma cell lines expressing Fyn (Figures 2, 3 and 5). Intriguingly, double knockdown of Fyn and Lyn induced caspase-8 activation and apoptosis in the mesothelioma cell lines expressing Fyn (Figure 5). These results suggest that Lyn plays a pivotal role in apoptosis of Fyn-deficient mesothelioma cells. We need to further investigate how Lyn and Fyn regulate apoptosis of mesothelioma cells.

Dasatinib is a highly potent Bcr-Abl kinase inhibitor used for the treatment of imatinib-resistant chronic myeloid leukemia (23). Dasatinib also inhibits SFK activity, leading to induction of apoptosis and cell cycle arrest and suppression of cell migration and invasion in mesothelioma cells (24). However, whether the apoptotic mechanism of dasatinib is the same as that of PP2 was not clear. We found that dasatinib inhibited SFK activity, reduced Lyn protein and induced apoptosis mediated by caspase-8 in NCI-H28 cells in a similar manner as PP2 (Figure 6). Recently, it has been reported that Src and Fyn are relevant targets for dasatinib action in lung cancer and that Lyn is a mediator of epithelial–mesenchymal transition and a target of dasatinib in breast cancer (25,26). These results suggest that dasatinib may be an effective molecular target drug against Fyn-deficient mesothelioma cells.

Preferential susceptibility to kinase inhibitor in NCI-H28 cells is also reported in c-Met, a receptor tyrosine kinase of hepatocyte growth factor, which is involved in cell growth, survival and migration (27). It has been shown that c-Met is overexpressed in NCI-H28 cells and that SU11274, a c-Met inhibitor, suppresses cell growth in NCI-H28 cells. If SU11274 induces reduction of Lyn protein in NCI-H28 cells, c-Met inhibitors as well as SFK inhibitors may induce apoptosis in Fyn-deficient mesothelioma cells.

In conclusion, SFK inhibitors, PP2 and dasatinib, reduce Lyn protein, leading to apoptosis mediated by caspase-8 in Fyn-deficient mesothelioma cells (Figure 6D). This study also shows potential utility of SFK inhibitors in the treatment of malignant mesothelioma and for the first time that deficiency of Fyn protein is prerequisite for apoptosis induced by SFK inhibitors in mesothelioma cells. Deficiency of Fyn protein would be a biomarker that discriminate the

sensitivity of SFK inhibitors in molecular-targeted therapy to mesothelioma. Additionally, further studies may open a novel way to develop therapy with both Fyn-deficiency and Lyn inhibition for this malignancy and other human tumor.

Funding

Grant-in-Aid for Scientific Research from Japan Society for the Promotion of Science (20590935).

Conflict of Interest Statement: None declared.

References

1. Robinson,B.W. *et al.* (2005) Malignant mesothelioma. *Lancet*, **366**, 397–408.
2. Tsao,A.S. *et al.* (2009) Malignant pleural mesothelioma. *J. Clin. Oncol.*, **27**, 2081–2090.
3. Vogelzang,N.J. (2008) Chemotherapy for malignant pleural mesothelioma. *Lancet*, **371**, 1640–1642.
4. Goudar,R.K. (2005) New therapeutic options for mesothelioma. *Curr. Oncol. Rep.*, **7**, 260–265.
5. Vogelzang,N.J. *et al.* (2003) Phase III study of pemetrexed in combination with cisplatin versus cisplatin alone in patients with malignant pleural mesothelioma. *J. Clin. Oncol.*, **21**, 2636–2644.
6. Yeatman,T.J. (2004) A renaissance for SRC. *Nat. Rev. Cancer*, **4**, 470–480.
7. Thomas,S.M. *et al.* (1997) Cellular functions regulated by Src family kinases. *Annu. Rev. Cell Dev. Biol.*, **13**, 513–609.
8. Mitra,S.K. *et al.* (2005) Focal adhesion kinase: in command and control of cell motility. *Nat. Rev. Mol. Cell Biol.*, **6**, 56–68.
9. Schlaepfer,D.D. *et al.* (2004) Control of motile and invasive cell phenotypes by focal adhesion kinase. *Biochim. Biophys. Acta*, **1692**, 77–102.
10. Cohen,G.M. (1997) Caspases: the executioners of apoptosis. *Biochem. J.*, **326**, 1–16.
11. Cursi,S. *et al.* (2006) Src kinase phosphorylates Caspase-8 on Tyr380: a novel mechanism of apoptosis suppression. *EMBO J.*, **25**, 1895–1905.
12. Jia,S.H. *et al.* (2008) Dynamic regulation of neutrophil survival through tyrosine phosphorylation or dephosphorylation of caspase-8. *J. Biol. Chem.*, **283**, 5402–5413.
13. Eguchi,R. *et al.* (2011) Arsenic trioxide induces apoptosis through JNK and ERK in human mesothelioma cells. *J. Cell. Physiol.*, **226**, 762–768.
14. Ingley,E. *et al.* (2006) Csk-binding protein mediates sequential enzymatic down-regulation and degradation of Lyn in erythropoietin-stimulated cells. *J. Biol. Chem.*, **281**, 31920–31929.
15. Lee,M. *et al.* (2004) Apoptotic effect of PP2 a Src tyrosine kinase inhibitor, in murine B cell leukemia. *J. Cell. Biochem.*, **93**, 629–638.
16. Liu,X. *et al.* (2010) The role of enoyl-CoA hydratase short chain 1 and peroxiredoxin 3 in PP2-induced apoptosis in human breast cancer MCF-7 cells. *FEBS Lett.*, **584**, 3185–3192.
17. De Toni,E.N. *et al.* (2007) P60-c-src suppresses apoptosis through inhibition of caspase 8 activation in hepatoma cells, but not in primary hepatocytes. *J. Hepatol.*, **46**, 682–691.
18. Saito,Y.D. *et al.* (2009) Fyn: a novel molecular target in cancer. *Cancer*, **116**, 1629–1637.
19. Sørensen,K.D. *et al.* (2008) Chromosomal deletion, promoter hypermethylation and downregulation of FYN in prostate cancer. *Int. J. Cancer*, **122**, 509–519.
20. Ban,K. *et al.* (2008) BCR-ABL1 mediates up-regulation of Fyn in chronic myelogenous leukemia. *Blood*, **111**, 2904–2908.
21. Grosso,S. *et al.* (2009) Gene expression profiling of imatinib and PD166326-resistant CML cell lines identifies Fyn as a gene associated with resistance to BCR-ABL inhibitors. *Mol. Cancer Ther.*, **8**, 1924–1933.
22. Scapini,P. *et al.* (2009) Multiple roles of Lyn kinase in myeloid cell signaling and function. *Immunol. Rev.*, **228**, 23–40.
23. Khoury,H.J. *et al.* (2009) Dasatinib treatment for Philadelphia chromosome-positive leukemias: practical considerations. *Cancer*, **115**, 1381–1394.
24. Tsao,A.S. *et al.* (2007) Inhibition of c-Src expression and activation in malignant pleural mesothelioma tissues leads to apoptosis, cell cycle arrest, and decreased migration and invasion. *Mol. Cancer Ther.*, **6**, 1962–1972.
25. Li,J. *et al.* (2010) A chemical and phosphoproteomic characterization of dasatinib action in lung cancer. *Nat. Chem. Biol.*, **6**, 291–299.
26. Choi,Y.-L.a *et al.* (2010) Lyn is a mediator of epithelial-mesenchymal transition and a target of dasatinib in breast cancer. *Cancer Res.*, **70**, 2296–2306.
27. Jagadeeswaran,R. *et al.* (2006) Functional analysis of c-Met/hepatocyte growth factor pathway in malignant pleural mesothelioma. *Cancer Res.*, **66**, 352–361.

Received October 1, 2011; revised January 23, 2012; accepted February 12, 2012

Original Paper

Cellular Physiology and Biochemistry

Cell Physiol Biochem 2012;29:667-674

Accepted: March 13, 2012

Mesothelioma Cell Proliferation through Autocrine Activation of PDGF-ββ Receptor

Miki Honda[1,2*], Takeshi Kanno[1*], Yumiko Fujita[1,2], Akinobu Gotoh[3], Takashi Nakano[2] and Tomoyuki Nishizaki[1]

[1]Division of Bioinformation, Department of Physiology, Hyogo College of Medicine, Nishinomiya, [2]Department of Thoracic Oncology, Hyogo College of Medicine, Nishinomiya, [3]Laboratory of Cell and Gene Therapy, Institute for Advanced Medical Sciences, Hyogo College of Medicine, Nishinomiya, *M. Honda and T. Kanno contributed equally to this work

Key Words

Malignant mesothelioma cell • Proliferation • PDGF-D • PDGF-ββ receptor

Abstract

Background/Aims: Growth factors play a critical role in proliferation for a variety of cancer cells. The present study was conducted to understand the signaling cascades underlying PDGF-D/PDGF-ββ receptor-mediated proliferation of mesothelioma cells. Methods: Cell growth and cell cycle were analyzed in human non-malignant Met5A cells and malignant mesothelioma cells such as MSTO-211H, NCI-H28, NCI-H2052, and NCI-H2452 cells. Results: Growth of all the cells used here was not affected by PDGF-D, regardless of concentrations (1-30 ng/ml) or treatment time (48-72 h). Spontaneous growth of those cells was significantly inhibited by knocking-down PDGF-D or PDGF-ββ receptor, without affecting cell cycling. The cell growth was significantly inhibited by the Akt inhibitor MK2206 and the ROCK inhibitor Y27632 for all the cell types, by the PDK1 inhibitor BX912 for NCI-H28 cells alone, and by the Rac1 inhibitor NSC23766 for NCI-H2052 cells alone, while the PI3 kinase inhibitor wortmannin had no effect. The cell growth, alternatively, was significantly attenuated by MAP kinase kinase inhibitor PD98059 or the ERK1/2 inhibitor FR180204 for all the cell types. Conclusion: The results of the present study show that PDGF-D promotes mesothelioma cell proliferation by targeting ROCK or MAP kinase through autocrine activation of PDGF-ββ receptor.

Introduction

Malignant mesothelioma is an aggressive and highly lethal tumor, which is caused by occupational exposure to asbestos fibres, particularly of the amphibole type [1]. Invasion into the mesothelium of the pleural cavity and/or the peritoneal cavity is commonly found with this tumor [1]. As is the case with other type of carcinoma cells, growth factors including platelet-derived growth factor (PDGF) serve as a pivotal mediator for proliferation of malignant mesothelioma cells too [2]. Lines of evidence have shown that PDGF, extracellularly secreted, stimulates malignant mesothelioma cell proliferation [3-8].

KARGER

Fax +41 61 306 12 34
E-Mail karger@karger.ch
www.karger.com

1015-8987/12/0296-0667$38.00/0

Accessible online at:
www.karger.com/cpb

Prof. Tomoyuki Nishizaki
Division of Bioinformation, Department of Physiology
Hyogo College of Medicine, 1-1 Mukogawa-cho, Nishinomiya 663-8501 (Japan)
Tel. +81-798-45-6397, Fax +81-798-45-6649
E-Mail tomoyuki@hyo-med.ac.jp

Of the PDGF family such as PDGF-A, -B, -C and -D, PDGF-A and –B are secreted as active dimers composed of single-domain protein chains (PDGF-AA and -BB). In contrast, PDGF-C and -D, which contain an N-terminal CUB and a conserved C-terminal growth factor domain, are secreted as a latent dimeric factor and undergo proteolytic processing at the hinge region between the CUB domain and the growth factor domain to produce the active form of PDGF-CC and -DD [9-11]. The serine protease tissue plasminogen activator (tPA) is a potent activator of latent dimeric PDGF-CC and the closely related protease urinary plasminogen activator (uPA), that is inhibited by plasminogen activator inhibitor-1 (PAI-1), activates latent PDGF-DD [12-14] (Fig. 1). PDGF receptors include three types of receptors such as PDGF-αα homodimer, PDGF-αβ heterodimer, and PDGF-ββ homodimer [9]. PDGF-αα and -αβ receptors are activated by PDGF-AA, -BB, and -CC, but PDGF-ββ is otherwise activated by PDGF-DD [9-11] (Fig. 1).

We have earlier found that PDGF-D secretion from malignant mesothelioma cells is stimulated by fetal bovine serum (FBS) and that urinary trypsin inhibitor (UTI), a potent inhibitor of uPA, inhibits FBS-induced migration of malignant mesothelioma cells [15], suggesting implication of PDGF-D/PDGF-ββ receptor in the migration. PDGF-ββ receptor contains the tyrosine kinase domain. When PDGF-ββ receptor is activated by PDGF-D, its own tyrosine kinase is inevitably activated, to phosphorylate insulin substrate protein (IRS)-1/-2 as a substrate. Phosphorylated IRS-1/-2, in turn, recruits and activates phosphoinositide 3-kinase (PI3 kinase), to produce phosphatidylinositol (3,4,5)-trisphosphate [PI (3,4,5) P_3] from phosphatidylinositol (4,5)-biphosphate [PI (4,5) P_2]. PI (3,4,5) P_3 binds to and activates phosphoinositide-dependent kinase-1 (PDK1), causing phosphorylation and activation of Akt. Akt activates the Rho family Rac1/Cdc42, followed by activation of the effector Rho-associated coiled-coil forming protein kinase (ROCK). For another pathway, activation of PDGF-ββ receptor/tyrosine kinase phosphorylates Shc2, that forms a complex of Shc2/Grb2/SOS to activate Ras. Ras subsequently activates Raf followed by the sequent phosphorylation and activation of mitogen-activated protein (MAP) kinase cascades such as MAP kinase kinase kinase (MEKK), MAP kinase kinase (MEK), and MAP kinase.

The present study investigated PDGF-D/PDGF-ββ receptor-mediated proliferation of human non-malignant Met5A cells and malignant mesothelioma cells such as MSTO-211H, NCI-H28, NCI-H2052, and NCI-H2452 cells. We show here that mesothelioma cell proliferation is regulated via a PDGF-D/PDGF-ββ receptor pathway.

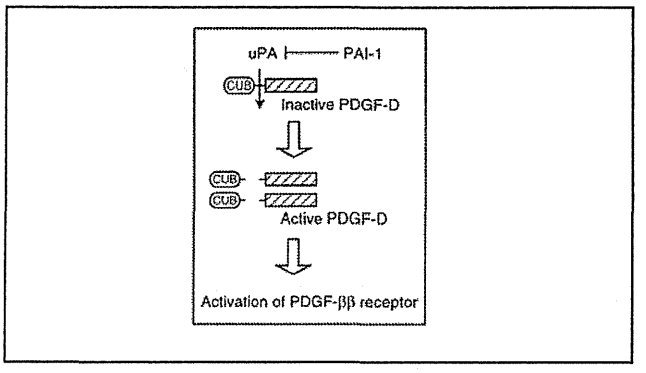

Fig. 1. Schematic regulatory pathway for production of the active form of PDGF-D.

Materials and Methods

Cell culture

Met5A, MSTO-211H, NCI-H28, NCI-H2052, and NCI-H2452 cell lines were purchased from American Type Culture Collection (Manassas, VA, USA). Cells were grown in RPMI-1640 medium supplemented with 10% (v/v) heat-inactivated FBS, 0.003% (w/v) L-glutamine, penicillin (final concentration, 100 U/ml), and streptomycin (final concentration, 0.1 mg/ml), in a humidified atmosphere of 5% CO_2 and 95% air at 37 °C.

Cell viability

Cell viability was assayed by the method using 3-(4,5-dimethyl-2-thiazolyl)-2,5-diphenyl-2H-tetrazolium bromide (MTT) as described previously [16]. MTT-reactive cells were quantified at an absorbance of 570 nm using a micro-plate reader (SPECTRAmax PLUS384, Molecular Devices, Sunnyvale, CA, USA).

Construction and transfection of small interfering RNA (siRNA)

The siRNAs silencing the PDGF-D-targeted gene (PDGF-D siRNA) or the PDGF receptor β subunit-targeted gene (PDGF-βR siRNA) were obtained from Cosmo Bio (Kyoto, Japan). The sequences of siRNAs used here were as follows: sense, 5'-CCA UCA AAG CUU UGC GCA ATT-3' and anti-sense, 5'-UUG CGC AAA GCU UUG AUG GTT-3'; sense, 5'-GGA AGU UCC UCC AAG GAU ATT-3' and anti-sense, 5'-UAU CCU UGG AGG AAC UUC CTT-3'; sense, 5'-GGU CAU ACC AUG ACC GGA ATT-3' and anti-sense, 5'-UUC CGG UCA UGG UAU GAC CTT-3' for PDGF-D; sense, 5'-GGA AUG A GG UGG UCA ACU UTT-3' and anti-sense, 5'-AAG UUG ACC ACC UCA UUC CTT-3'; sense, 5'-GCU CAU GGC CUG AGC CAU UTT-3' and anti-sense, 5'-AAU GGC UCA GGC CAU GAG CTT-3'; and sense, 5'-GAG AGG ACC UGC CGA GCA ATT-3' and anti-sense, 5'-UUG CUC GGC AGG UCC UCU CTT-3' for PDGF-ββ

receptor. Negative control siRNA (NC siRNA) was purchased from Santa Cruz Biotechnology (Santa Cruz, CA, USA). The PDGF-D siRNA, the PDGF-βR siRNA, and the NC siRNA were reverse-transfected into cells using a Lipofectamine LTX (Invitrogen, Carlsbad, CA, USA). Cells were used for experiments 48 h after transfection.

Reverse transcription-polymerase chain reaction (RT-PCR)

Total RNAs were purified from cells, transfected with the NC siRNA, the PDGF-D siRNA or the PDGF-βR siRNA, by an acid/guanidine/thiocyanate/chloroform extraction method using a Sepasol-RNA I Super kit (Nacalai, Kyoto, Japan). After purification, total RNAs were treated with RNase free-DNase I (2 units) at 37 °C for 30 min to remove genomic DNAs, and 10 μg of RNAs were resuspended in water. Then, oligo dT primers, dNTPs, 5x First Strand buffer, and SuperScripit III RNase H-Reverse Transcriptase were added to the RNA solution and incubated at 65 °C for 5 min followed by 56 °C for 60 min, 58 °C for 60 min, 85 °C for 5 min to synthesize the first strand cDNA. Subsequently, 1 μl of the reaction solution was diluted with water and mixed with 10x PCR reaction buffer, dNTPs, $MgCl_2$, oligonucleotide, dimethylsulfoxide [final concentration, 5% (v/v)] and 1 unit of Taq polymerase (Fermentas, St. Leon-Roth, Germany)(final volume, 20 μl). RT-PCR was carried out with a GeneAmp PCR system model 9600 DNA thermal cycler (Applied Biosystems, Indianapolis, IN, USA) programmed as follows: the first one step, 94 °C for 4 min and the ensuing 30 cycles, 94 °C for 1 s, 62 °C for 15 s, and 72 °C for 30 s. The primers used here were as follows: 5'-TAA TGT ATC TTG CTT TTG TGT TCC CGT CTT-3' and 5'-CCT TTA AAA CAG ACA CAA AGG AGG CAG AG-3' for PDGF-D; 5'-CGA GTG GAC ATA CCC CCG CAA-3' and 5'-CAG CAC TCG GAC AGG GAC ATT GAT-3' for the PDGF receptor β subunit; and 5'-GAC TTC AAC AGC GAC ACC CAC TCC-3' and 5'-AGG TCC ACC ACC CTG TTG CTG TAG-3' for GAPDH. PCR products were stained with ethidium bromide and visualized by 2% (w/v) agarose gel electrophoresis.

Real-time RT-PCR

Total RNAs of cells were purified by an acid/guanidine/thiocyanate/chloroform extraction method using the Sepasol-RNA I Super kit. After purification, total RNAs were treated with RNase-free DNase I (2 units) at 37 °C for 30 min to remove genomic DNAs, and 10 μg of RNAs was resuspended in water. Then, random primers, dNTP, 10x RT buffer, and Multiscribe Reverse Transcriptase were added to an RNA solution and incubated at 25 °C for 10 min followed by 37 °C for 120 min to synthesize the first-strand cDNA. Real-time RT-PCR was performed using a SYBR Green Realtime PCR Master Mix (Takara Bio, Otsu, Japan) and the Applied Biosystems 7900 real-time PCR detection system. Thermal cycling conditions were as follows: first step, 94 °C for 4 min; the ensuing 40 cycles, 94 °C for 1 s, 65 °C for 15 s, and 72 °C for 30 s. The expression level of each mRNA was normalized by that of GAPDH mRNA. Primers used for real-time RT-PCR are 5'-GCC CTG CCT GCC CTG GAA C-3' and 5'-ACG ATG TAG TCC TCC TTC TTT GGG TAA TC-3' for uPA; 5'-CCC ACC GCC GCC TCT TCC-3' and 5'-CAT GTC GGT CAT TCC CAG GTT CTC TA-3' for PAI-1; and 5'-GAC TTC AAC AGC GAC ACC CAC TCC-3' and 5'-AGG TCC ACC ACC CTG TTG CTG TAG- 3' for GAPDH.

Cell cycle analysis

Cells were harvested by a trypsinization 48 h after transfection with the NC siRNA or the PDGF-βR siRNA, fixed with 70% (v/v) ethanol at 4 °C overnight. Fixed cells were incubated in phosphate-buffered saline containing 1.5 μg/ml RNase A for 1 h at 37 °C, followed by staining with 5 μl of propidium iodide (PI) for 20 min on ice. Then, cells were collected on a nylon mesh filter (pore size, 40 μm), and cell cycles were assayed using a flowcytometer (FACSCalibur, Becton Dickinson, USA) at an excitation of 488 nm and an emission of 585 nm, and analyzed using a Mod Fit LT software (Verity Software House Inc., Topshan, USA).

Statistical analysis

Statistical analysis was carried out using Dunnett's test.

Results

Mesothelioma cell growth in a PDGF-D- and PDGF-ββ receptor-dependent manner

Growth of non-malignant Met5A cells and malignant MSTO-211H, NCI-H28, NCI-H2052, and NCI-H2452 cells was not affected by 48-h treatment with exogenous PDGF-D at concentrations ranging from 1 to 30 ng/ml (Fig. 2A) or treatment with exogenous PDGF-D at 10 ng/ml for 48-72 h (Fig. 2B).

To examine whether endogenous PDGF-D regulates mesothelioma cell growth, the PDGF-D siRNA was constructed and transfected into cells. Expression of the PDGF-D mRNA for cells transfected with the PDGF-D siRNA was clearly suppressed as compared with the expression for cells transfected with the NC siRNA (Fig. 3A), confirming PDGF-D knock-down. For all the cell types used here, growth of cells transfected with the PDGF-D siRNA was significantly inhibited as compared with cells transfected with the NC siRNA (Fig. 3A). This suggests regulation of mesothelioma cell proliferation by endogenous PDGF-D.

If this is true, then PDGF-ββ receptor, that is activated by the active form of PDGF-D, should be implicated in the regulation of mesothelioma cell proliferation. To address this point, the PDGF-βR siRNA was constructed and transfected into cells. Expression of the PDGF receptor-β subunit mRNA for cells transfected with the PDGF-βR siRNA was abrogated (Fig. 3B), confirming PDGF-ββ receptor knock-down. Expectedly, spontaneous cell growth for all the cell types

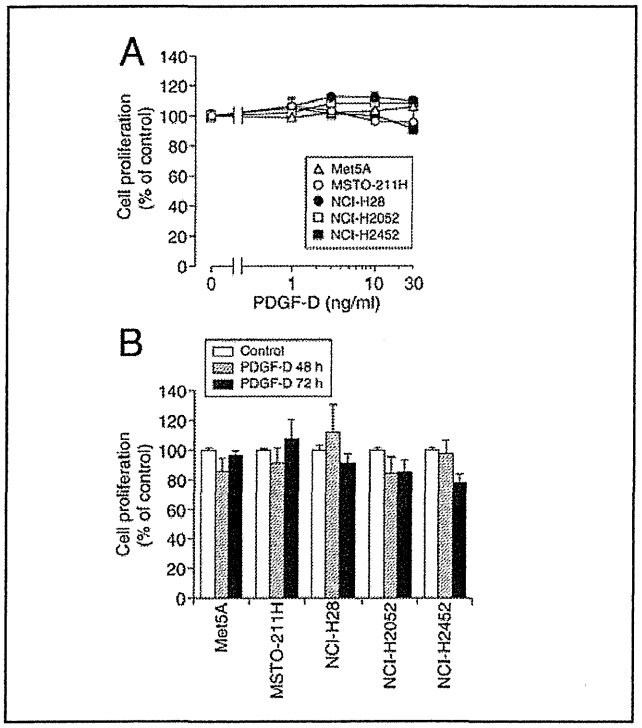

Fig. 2. The effect of exogenously applied PDGF-D on mesothelioma cell proliferation. (A) Met5A, MSTO-211H, NCI-H28, NCI-H2052, and NCI-H2452 cells were treated with PDGF-D at concentrations as indicated for 48 h, and then MTT assay was carried out. In the graph, each point represents the mean (± SEM) percentage of control (MTT intensities before PDGF-D treatment)(n=4 independent experiments). (B) Cells were treated with 10 ng/ml of PDGF-D for 48-72 h followed by MTT assay. In the graph, each column represents the mean (± SEM) percentage of control (MTT intensities before PDGF-D treatment)(n=4 independent experiments).

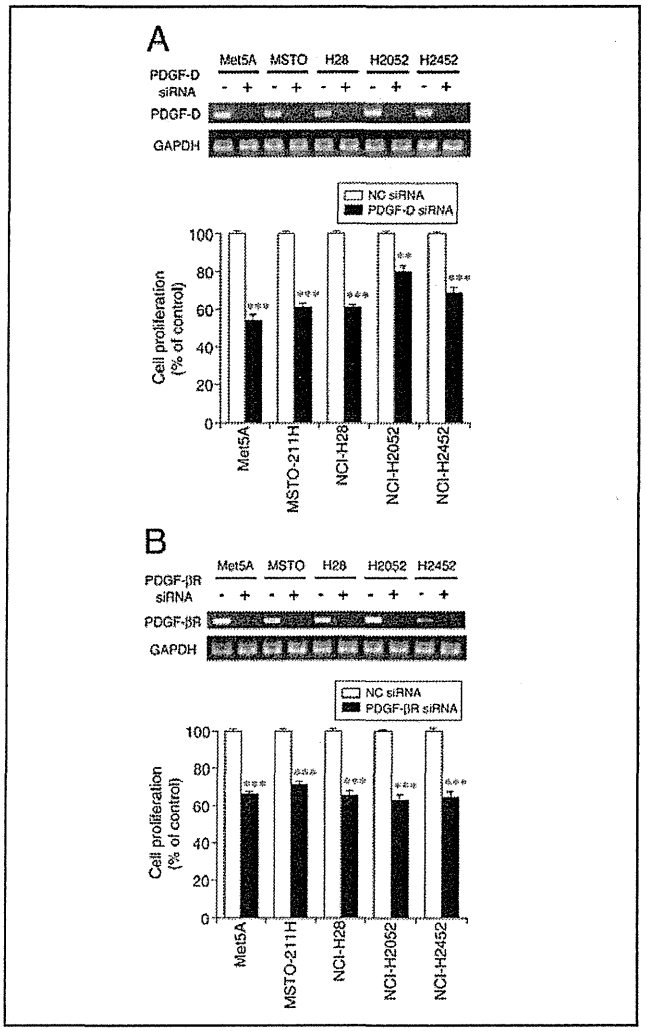

Fig. 3. Mesothelioma cell proliferation via a PDGF-D/PDGF-ββ receptor pathway. (A) Met5A, MSTO-211H (MSTO), NCI-H28 (H28), NCI-H2052 (H2052), and NCI-H2452 cells (H2452) were transfected with the NC siRNA [PDGF-D siRNA (-)] or the PDGF-D siRNA [PDGF-D siRNA (+)] followed by RT-PCR 48 h after transfection. Then, MTT assay was carried out 96 h after transfection. PCR products for PDGF-D and GAPDH are shown in the upper column. Note that the PDGF-D mRNA signal was not visible for cells transfected with the PDGF-D siRNA. In the graph, each column represents the mean (± SEM) percentage of control (MTT intensities for cells transfected with the NC siRNA)(n=6 independent experiments). $^{**}P<0.001$; $^{***}P<0.0001$ as compared with control, Dunnett's test. (B) Cells as indicated was transfected with the NC siRNA [PDGF-βR siRNA (-)] or the PDGF-βR siRNA [PDGF-βR siRNA (+)], followed by RT-PCR 48 h after transfection and MTT assay 96 h after transfection. PCR products for PDGF-βR and GAPDH in RT-PCR are shown in the upper column. Note that the PDGF-βR mRNA signal was not detectable for cells transfected with the PDGF-βR siRNA. In the graph, each column represents the mean (± SEM) percentage of control (MTT intensities for cells transfected with the NC siRNA)(n=6 independent experiments). $^{***}P<0.0001$ as compared with control, Dunnett's test.

was significantly attenuated by knocking-down PDGF-ββ receptor (Fig. 3B). In contrast, each phase of cell cycling for all the cell types was not influenced by knocking-down PDGF-ββ receptor (Fig. 4). Taken together, these results indicate that endogenous PDGF-D promotes mesothelioma cell proliferation by activating PDGF-ββ receptor, without affecting cell cycle.

Mesothelioma cell proliferation under the control of ROCK and MAP kinase

For all the cell types examined here, spontaneous cell growth was significantly inhibited by MK2206 (5 μM), an inhibitor of Akt (Fig. 5C), or Y27632 (10 μM), an inhibitor of ROCK, with the highest potential (Fig. 5E). BX912 (100 nM), an inhibitor of PDK1, and NSC23766 (1 μM), an inhibitor of Rac1, significantly attenuated the

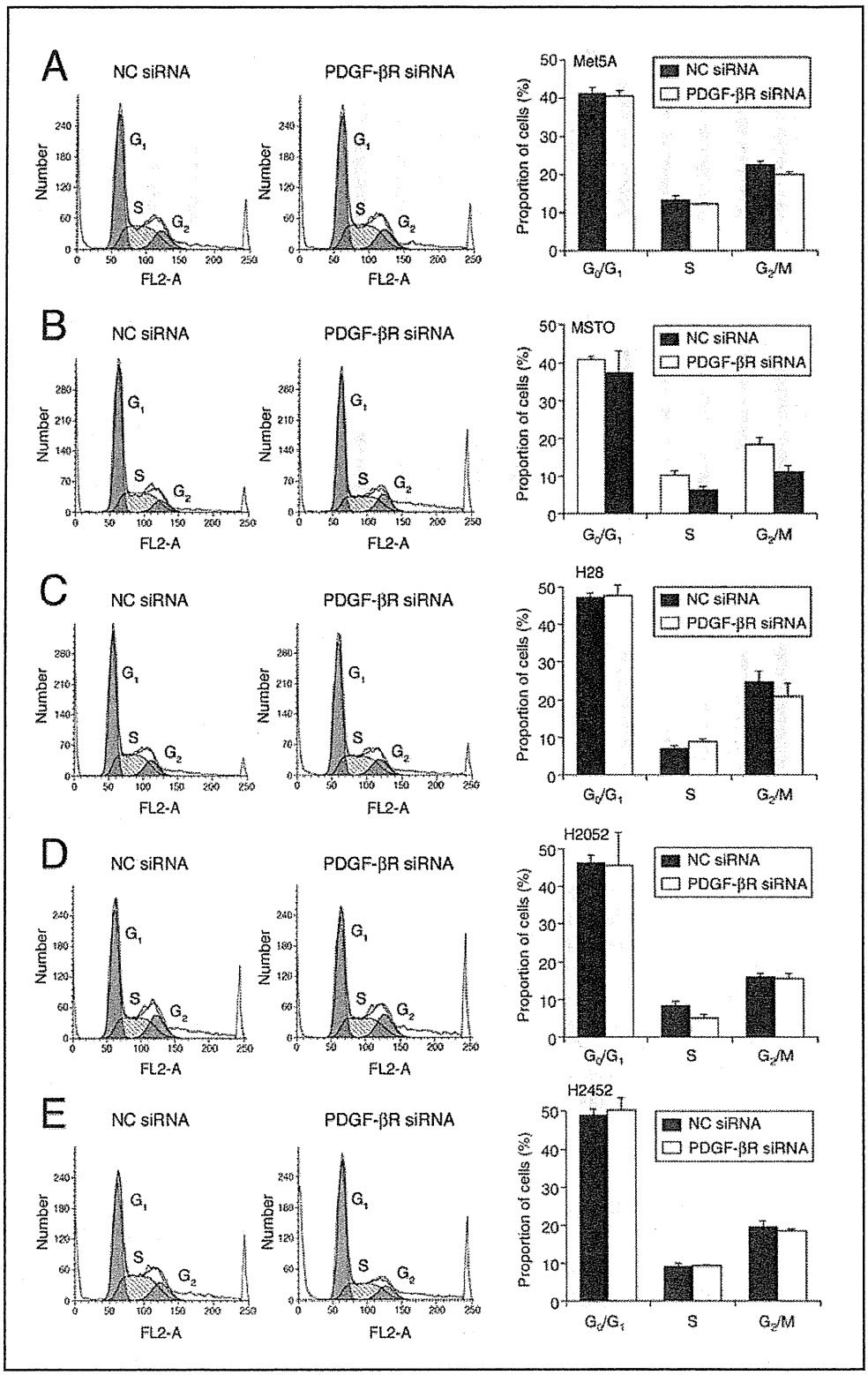

Fig. 4. The effect of PDGF-ββ receptor knock-down on cell cycling. Met5A (A), MSTO-211H (MSTO)(B), NCI-H28 (H28)(C), NCI-H2052 (H2052)(D), and NCI-H2452 cells (H2452)(E) were transfected with the NC siRNA or the PDGF-βR siRNA, and 96 h later cell cycle analysis was carried out. Typical profiles are shown in the left panel. In the graphs, each column represents the mean (± SEM) percentage for phases of cell cycling (n=4 independent experiments).

cell growth for NCI-H28 cells alone (Fig. 5B) and for NCI-H2052 cells alone (Fig. 5D), respectively, but wortmannin (10 μM), an inhibitor of PI3 kinase, had no effect (Fig. 5A). This indicates that spontaneous mesothelioma cell proliferation is regulated by ROCK, a signaling cascade downstream PDGF-ββ receptor. This also suggests that ROCK is unlikely activated via a well-recognized pathway along a PI3 kinase/PDK1/

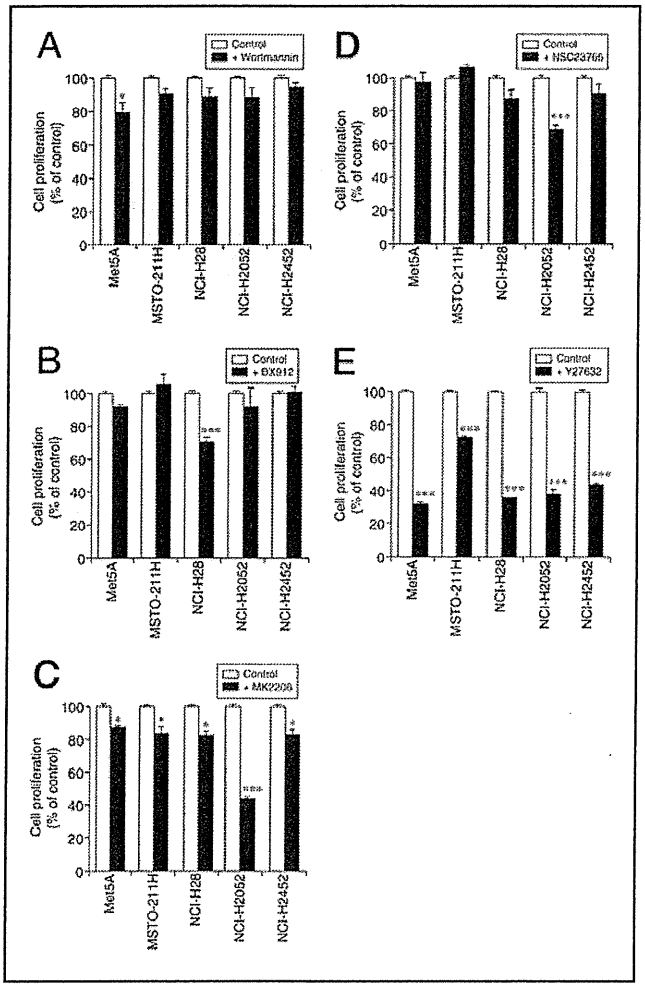

Fig. 5. The effect of inhibitors for PI3 kinase, PDK1, Akt, Rac1, and ROCK on mesothelioma cell proliferation. Cells as indicated were incubated in the absence (Control) and presence of wortmannin (10 μM), BX912 (100 nM), MK2206 (5 μM), NSC23766 (1 μM), or Y27632 (10 μM) for 48 h, and then, MTT assay was carried out. In the graph, each column represents the mean (± SEM) percentage of control (MTT intensities in the absence of inhibitors)(n=6 independent experiments). *P<0.01; **P<0.001; ***P<0.0001 as compared with control, Dunnett's test.

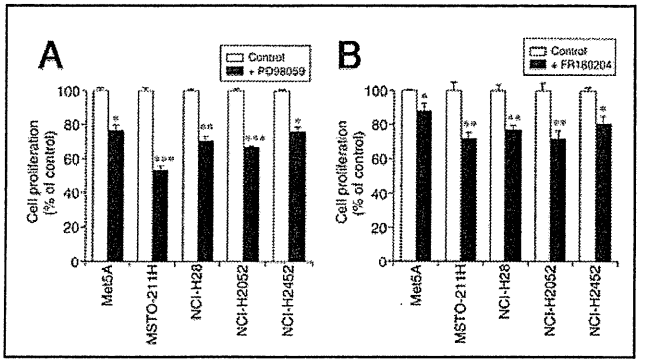

Fig. 6. The effect of inhibitors for MEK and ERK1/2 on mesothelioma cell proliferation. Cells as indicated were incubated in the absence (Control) and presence of PD98059 (50 μM), or FR180204 (10 μM) for 48 h, and then, MTT assay was carried out. In the graph, each column represents the mean (± SEM) percentage of control (MTT intensities in the absence of inhibitors)(n=6 independent experiments). *P<0.01; **P<0.001; ***P<0.0001 as compared with control, Dunnett's test.

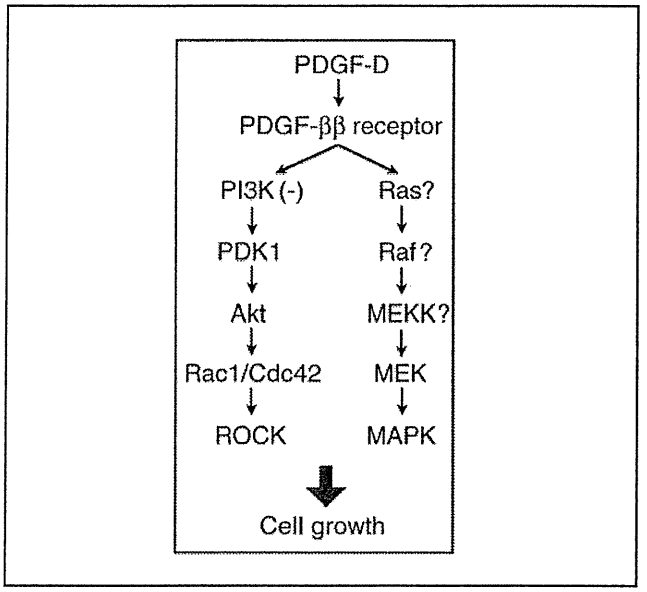

Fig. 7. Putative PDGF-D/PDGF-ββ receptor signaling pathways for mesothelioma cell proliferation. MEKK, MEK kinase; MAPK, MAP kinase.

Akt/Rac1 (Cdc42)/ROCK axis linked to PDGF-ββ receptor (Fig. 7).

The cell growth, on the other hand, was significantly prevented by PD98059 (50 μM), an inhibitor of MEK (Fig. 6A), or FR180204 (10 μM), an inhibitor of the MAP kinase ERK1/2, for all the cell types (Fig. 6B). This indicates that MEK/ERK also participates in spontaneous mesothelioma cell proliferation, although it has not been examined yet whether those kinases are activated via a pathway along a Ras/Raf/MEKK/MEK/MAP kinase downstream PDGF-ββ receptor (Fig. 7).

Higher expression of the uPA mRNA in malignant mesothelioma cells

uPA produces the active form of PDGF-D to activate PDGF-ββ receptor through proteolytic processing, but PAI-1 inhibits the uPA action (Fig. 1). Expression of the uPA mRNA in malignant mesothelioma cells such as

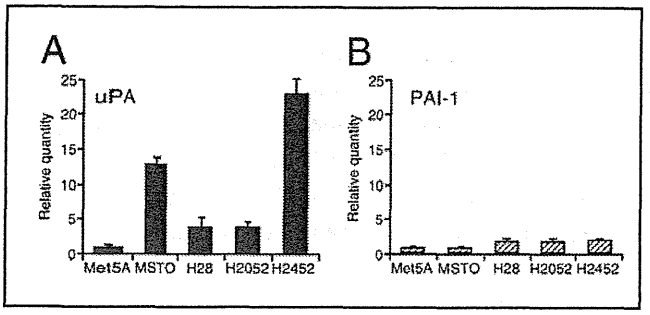

Fig. 8. Expression of mRNAs for uPA (A) and PAI-1 (B). Real-time RT-PCR was carried out in Met5A, MSTO-211H (MSTO), NCI-H28 (H28), NCI-H2052 (H2052), and NCI-H2452 cells (H2452). In the graphs, each column represents the mean (± SEM) ratio against mRNA intensities for Met5A cells (n=4 independent experiments).

MSTO-211H, NCI-H28, NCI-H2052, and NCI-H2452 cells was much higher than the expression in non-malignant Met5A cells (Fig. 8A). In contrast, there was no big difference in the expression of the PAI-1 mRNA between malignant and non-malignant mesothelioma cells (Fig. 8B). In our earlier study, expression of PDGF-ββ receptor in malignant mesothelioma cells was significantly higher than the expression in Met5A cells, although no difference in PDGF-D expression was found between them [15]. Collectively, these results suggest that the active form of PDGF-D, to activate PDGF-ββ receptor, is produced more in malignant mesothelioma cells than in non-malignant Met5A cells.

Discussion

In the present study, exogenous PDGF-D had no effect on proliferation for Met5A non-malignant mesothelioma cells and malignant mesothelioma cells such as MSTO-211H, NCI-H28, NCI-H2052, and NCI-H2452 cells, regardless of its concentrations and its treatment time. Amazingly, spontaneous cell growth was inhibited by knocking-down PDGF-D or PDGF-ββ receptor for all the cell types examined here. In contrast, cell cycling for all the cell types was not altered by knocking-down PDGF-ββ receptor. It is indicated from these results that endogenous PDGF-D, extracellularly secreted, promotes mesothelioma cell proliferation by activating PDGF-ββ receptor, without affecting cell cycling. This also suggests that PDGF-ββ receptor in mesothelioma cells is sufficiently activated to the maximal levels by endogenous PDGF-D, i.e., no further activation of the receptor is obtained with exogenously applied PDGF-D.

PDGF-ββ receptor engages two major signaling pathways; a pathway along a PI3 kinase/PDK1/Akt/Rac1 (Cdc42)/ROCK axis and another along a Ras/Raf/MEKK/MEK/MAP kinase axis (Fig. 7). For all the cell types, spontaneous cell growth was prevented by the Akt inhibitor MK2206, to a smaller extent except for NCI-H2052 cells, or the ROCK inhibitor Y27632, to a greater extent. Then, one would think that ROCK is activated via the former pathway downstream PDGF-ββ receptor. An unexpected result, however, was that no inhibition of the cell growth for all the cell types was obtained with the PI3 kinase inhibitor wortmannin. This denies the participation of PI3 kinase at the initial entrance for a pathway along a PI3 kinase/PDK1/Akt/Rac1 (Cdc42)/ROCK axis. Furthermore, the PDK1 inhibitor BX912 suppressed the cell growth for NCI-H28 cells alone or the Rac1 inhibitor NSC23766 attenuated it for NCI-H2052 cells alone. Overall, these results indicate that ROCK as a downstream target of PDGF-ββ receptor plays a crucial role in spontaneous mesothelioma cell proliferation but that ROCK may be activated via a pathway independent of a PI3 kinase/PDK1/Akt/Rac1 (Cdc42) axis, i.e., via an as of yet unknown pathway.

Spontaneous mesothelioma cell growth, alternatively, was significantly prevented by the MEK inhibitor PD98059 or the ERK1/2 inhibitor FR180204 for all the cell types. This suggests that MEK/MAP kinase is another downstream target of PDGF-ββ receptor responsible for spontaneous mesothelioma cell proliferation, although the implication of Ras, Raf, and MEKK in the activation of MEK and MAP kinase has not been ascertained here. How ROCK is activated in mesothelioma cells also remains to be explored. A plausible explanation for this is that ROCK might be activated by a MAP kinase cascade, regardless of PI3 kinase, PDK1, Akt, or Rac1 (Cdc42). To address this question, we are currently attempting further experiments.

In the present study, malignant mesothelioma cells more highly expressed the uPA mRNA than non-malignant Met5A cells, while there was no difference in the expression of the PAI-1 mRNA between malignant and non-malignant mesothelioma cells. This, taken together with the fact that much higher expression of PDGF-ββ receptor is found in malignant mesothelioma cells as compared with in non-malignant mesothelioma cells, with

no difference in the expression of PDGF-D between them [15], raises the possibility that uPA-mediated production of the active form of PDGF-D from the inactive form of PDGF-D in malignant mesothelioma cells is greater than in non-malignant mesothelioma cells, to endogenously activate PDGF-ββ receptor. The expression levels of uPA, therefore, may be a critical index to determine malignancy for mesothelioma cells.

In conclusion, the results of the present study show that PDGF-D promotes mesothelioma cell proliferation by activating ROCK via a pathway independent of PI3 kinase/PDK1/Akt/Rac1 (Cdc42) axis or MAP kinase, possibly along a Ras/Raf/MEKK/MEK axis, through autocrine activation of PDGF-ββ receptor. The former may represent a novel pathway for mesothelioma cell proliferation.

References

1 Nakano T: Malignant mesothelioma-diagnosis and treatment strategies. Gan To Kagaku Ryoho 2006;33:1215-1220.
2 Halper J: Growth factors as active participants in carcinogenesis: a perspective. Vet Pathol 2010;47:77-97.
3 Garlepp MJ, Leong CC: Biological and immunological aspects of malignant mesothelioma. Eur Respir J 1995;8:643-650.
4 Upham JW, Garlepp MJ, Musk AW, Robinson BW: Malignant mesothelioma: new insights into tumour biology and immunology as a basis for new treatment approaches. Thorax 1995;50:887-893.
5 Filiberti R, Marroni P, Neri M, Ardizzoni A, Betta PG, Cafferata MA, Canessa PA, Puntoni R, Ivaldi GP, Paganuzzi M: Serum PDGF-AB in pleural mesothelioma. Tumour Biol 2005;26:221-226.
6 Versnel MA, Hagemeijer A, Bouts MJ, van der Kwast TH, Hoogsteden HC: Expression of *c-sis* (PDGF B-chain) and PDGF A-chain genes in ten human malignant mesothelioma cell lines derived from primary and metastatic tumors. Oncogene 1988;2:601-605.
7 Gerwin BI, Lechner JF, Reddel RR, Roberts AB, Robbins KC, Gabrielson EW, Harris CC: Comparison of production of transforming growth factor-β and platelet-derived growth factor by normal human mesothelial cells and mesothelioma cell lines. Cancer Res 1987;47:6180-6184.
8 Van der Meeren A, Seddon MB, Betsholtz CA, Lechner JF, Gerwin BI: Tumorigenic conversion of human mesothelial cells as a consequence of platelet-derived growth factor-A chain overexpression. Am J Respir Cell Mol Biol 1993;8:214-221.
9 Alvarez RH, Kantarjian HM, Cortes JE: Biology of platelet-derived growth factor and its involvement in disease. Mayo Clin Proc 2006;81:1241-1257.
10 Bergsten E, Uutela M, Li X, Pietras K, Ostman A, Heldin CH, Alitalo K, Eriksson U: PDGF-D is a specific, protease-activated ligand for the PDGF β-receptor. Nat Cell Biol 2001;3:512-516.
11 Fredriksson L, Ehnman M, Fieber C, Eriksson U: Structural requirements for activation of latent platelet-derived growth factor CC by tissue plasminogen activator. J Biol Chem 2005;280:26856-26862.
12 Ehnman M, Li H, Fredriksson L, Pietras K, Eriksson U: The uPA/uPAR system regulates the bioavailability of PDGF-DD: implications for tumour growth. Oncogene 2009;28:534-544.
13 Fredriksson L, Li H, Fieber C, Li X, Eriksson U: Tissue plasminogen activator is a potent activator of PDGF-CC. EMBO J 2004;23:3793-3802.
14 Ustach CV, Kim HR: Platelet-derived growth factor D is activated by urokinase plasminogen activator in prostate carcinoma cells. Mol Cell Biol 2005;25:6279-6288.
15 Yaguchi T, Muramoto M, Nakano T, Nishizaki T: Urinary trypsin inhibitor suppresses migration of malignant mesothelioma. Cancer Lett 2010;288:214-218.
16 Yaguchi T, Saito M, Yasuda Y, Kanno T, Nakano T, Nishizaki T: Higher concentrations of extracellular ATP suppress proliferation of Caco-2 human colonic cancer cells via an unknown receptor involving PKC inhibition. Cell Physiol Biochem 2010;26:125-134.

Ann Surg Oncol (2012) 19:4229–4237
DOI 10.1245/s10434-012-2506-0

Annals of
SURGICAL ONCOLOGY
OFFICIAL JOURNAL OF THE SOCIETY OF SURGICAL ONCOLOGY

ORIGINAL ARTICLE – THORACIC ONCOLOGY

Circulating Endothelial Cell (CEC) as a Diagnostic and Prognostic Marker in Malignant Pleural Mesothelioma (MPM)

Kazue Yoneda, BA[1], Fumihiro Tanaka, MD, PhD[1,5], Nobuyuki Kondo, MD, PhD[1], Hayato Orui, MD[1], Masaki Hashimoto, MD[1], Teruhisa Takuwa, MD[1], Seiji Matsumoto, MD, PhD[1], Yoshitomo Okumura, MD, PhD[1,6], Noriaki Tsubota, MD, PhD[2], Ayuko Sato, PhD[3], Tohru Tsujimura, MD, PhD[3], Kozo Kuribayashi, MD, PhD[4], Kazuya Fukuoka, MD, PhD[4], Takashi Nakano, MD, PhD[4], and Seiki Hasegawa, MD, PhD[1]

[1]Department of Thoracic Surgery, Hyogo College of Medicine, Nishinomiya, Japan; [2]Department of Thoracic Oncology, Hyogo College of Medicine, Nishinomiya, Japan; [3]Department of Pathology, Hyogo College of Medicine, Nishinomiya, Japan; [4]Division of Respiratory Medicine, Department of Internal Medicine, Hyogo College of Medicine, Nishinomiya, Japan; [5]Second Department of Surgery (Chest Surgery), University of Occupational and Environmental Health, Kitakyusyu, Japan; [6]Department of Thoracic Surgery, Itami City Hospital, Itami, Japan

ABSTRACT

Background. The purpose of this study was to investigate the diagnostic and prognostic value of circulating endothelial cell (CEC), a potential surrogate of tumor angiogenesis, in malignant pleural mesothelioma (MPM).

Methods. We prospectively evaluated CEC count in 4.0 mL of peripheral blood sampled from patients with a suspicion of MPM. An automated system was used to capture CECs with an anti-CD146 antibody.

Results. Of 109 eligible patients, 30 were finally diagnosed with non-malignant diseases, and 79 were with MPM. CEC count was significantly higher in MPM patients than in NM patients (mean CEC count, 120.3 and 39.9, respectively; $P = 0.001$), and a receiver operating characteristic (ROC) curve analysis showed that CEC provided a significant diagnostic performance in discrimination between MPM and nonmalignant diseases with an area under curve (AUC–ROC) of 0.700 (95 % confidence interval [95 % CI], 0.595–0.806; $P = 0.001$). Among MPM patients, CEC count was positively correlated with intratumoral microvessel density (MVD), a measurement of tumor angiogenesis (Spearman correlation coefficiency [r] = 0.444; $P = 0.001$). Higher CEC count (>50) was significantly associated with a poor prognosis (median overall survival, 11.4 months [95 % CI, 7.6–15.2] for higher CEC count patients versus 20.1 months [95 % CI, 16.0–24.2] for lower CEC count patients; $P = 0.028$). A multivariate analysis showed that higher CEC count was a significant and independent factor to predict a poor prognosis (hazard ratio [HR], 2.24, [95 % CI, 1.24–4.43]; $P = 0.009$).

Conclusions. CEC, as a surrogate of tumor angiogenesis, was a promising marker in diagnosis and prediction of prognosis in MPM.

Malignant pleural mesothelioma (MPM) is a highly aggressive malignant tumor of the pleura associated with asbestos exposure.[1–3] The gold standard for the diagnosis is histological examination, which usually needs invasive procedures such as core-needle biopsy or video-assisted thoracoscopic (VATS) biopsy.[3,4] Such invasive procedures are not feasible for mass screening for asbestos-exposed high-risk population or may not be performed for patients with poor performance status (PS). Accordingly, it is clinically important to develop and establish noninvasive diagnostic procedures to accurately predict and/or exclude the diagnosis of MPM. A number of noninvasive markers have merged and have been evaluated, in accordance with recent advances in understanding molecular and biological characteristics of MPM.[5,6] Among them, serum soluble mesothelin-related protein (SMRP) is the most promising diagnostic marker in discrimination of MPM from non-malignant diseases or from other malignant diseases.[5] However, the use of SMRP in daily clinical practice is not

Part of this study was presented at the 47th Annual Meeting of the American Society of Clinical Oncology, June 3–7, 2011, Chicago, IL.

First Received: 22 April 2012;
Published Online: 24 July 2012

F. Tanaka, MD, PhD
e-mail: ftanaka@med.uoeh-u.ac.jp

recommended, as no prospective validation study has confirmed the diagnostic performance.[4,5,7]

MPM is a uniformly fatal disease with a median survival time of 4–12 months, as there is no established treatment modality for the cure.[2,8–10] In addition to lack of effective treatment options, lack of useful clinical indicators predicting prognosis and/or response to treatment may contribute to the poor prognosis.[5]

Angiogenesis plays an essential role in development and progression of a variety of malignant tumors.[11] As MPM is characterized by aggressive angiogenesis, angiogenesis is a promising therapeutic target and can be a useful clinical marker.[12] In fact, some previous studies showed that microvessel density (MVD), a measurement of tumor angiogenesis, provided a significant prognostic value in MPM.[13–15] Despite such potential usefulness, MVD has not been established as a practical clinical marker partly due to lack of accuracy and/or reproducibility. In addition, an invasive procedure such as VATS biopsy is required for evaluation of MVD in tumor tissues. Thus, there is a great need for noninvasive markers that reflect tumor angiogenesis.

Circulating endothelial cells (CECs) are endothelial cells that shed from the vascular wall and circulate in the peripheral blood. It is well known that CECs are increased along with extent of vascular damage in cardiovascular diseases, vasculitis, and infectious diseases.[16,17] CECs are also increased in a variety of malignant tumors including breast, colorectal, lung, prostate, head and neck, ovarian, and renal cell carcinoma, and CECs can be decreased in response to anti-angiogenic treatment.[16–21] These results may indicate that CECs play an important role in development and progression of malignant tumors and suggest that CEC, as a noninvasive angiogenesis marker, can be potentially useful for diagnosis and decision-making in therapy of malignant tumors. However, no previous study on CEC in MPM has been reported. Thus, in the present study, we quantitatively evaluated CECs with an automated system and prospectively examined its diagnostic performance and prognostic value in MPM.

PATIENTS AND METHODS

Study Design

Patients who presented at the Hyogo College of Medicine (HCM) Hospital to receive pleural biopsy with a suspicion of MPM on computed tomography (CT) and positron emission tomography (PET) scanning were eligible. Patients who had concurrent or prior malignancy treated within in the previous 5 years were excluded. In addition, patients who have uncontrolled ischemic heart disease, systemic vasculitis, infectious disease, or diabetes were excluded. All patients provided written informed consent before enrollment.

Peripheral blood (4.0 mL) was collected from each patient and was served for evaluation of CECs. Complete clinical data including history, physical examination, laboratory, and radiographic studies were also collected. For all patients, pleural biopsy was performed, and final pathological diagnosis was established. For patients with MPM, whole-body CT as well as brain CT or magnetic resonance imaging (MRI) were routinely conducted to evaluate tumor progression. Clinical (c-) stage was determined according to the current tumor-node-metastasis (TNM) classification as determined by the International Mesothelioma Interest Group (IMIG).[22] This study was approved by the Institutional Review Board of HCM.

Evaluation of CECs

CECs were isolated from peripheral blood using the CellTracks system (Veridx LLC, Raritan, NJ), and the number of CECs was determined following a manufacturer's protocol as described previously.[20] In brief, endothelial cells were immunomagnetically captured using ferroparticles coated with anti-CD146 antibodies. The enriched samples were then stained with the 4′,6-diamidino-2-phenylindole (DAPI), an anti-CD105 antibody conjugated to phy-coerythrin (CD105-PE), and an anti-CD45 antibody conjugated to allophycocyanin (CD45-APC). Stained cells were then analyzed on a fluorescent microscope using the Cell Track Analyzer II (Veridex LLC). Contaminated white blood cells were excluded by negative selection for CD45, and the criteria for each cell to be defined as a CEC were: a visible DAPI-positive nucleus, positive CD105-staining in the cytoplasm, and negative staining for CD45. All evaluations were performed by two authors (K.Y. and F.T., both completed the "Cell Interpretation Proficiency Assessment" managed by the Veridex LL) independently without knowledge of clinical characteristics of patients.

Evaluation of Tumor Angiogenesis (MVD)

Evaluation of tumor angiogenesis was performed in MPM patients, when adequate biopsy specimens, which were suitable for the following immunohistochemical staining (IHC) evaluation, were available. IHC with an anti-CD34 antibody QBEnd10 (mouse IgG1 k, 50 mg/mL; DAKO Japan, Tokyo, Japan) to highlight endothelial cells was performed using an automated staining system (ChemMate EnVision Detection kit and DAKO Autostainer system; DAKO Japan) following the manufacturer's protocol. The 10 most vascular areas within a section were selected for quantitation of angiogenesis, and vessels

TABLE 1 Characteristics of patients

	Nonmalignant disease		Malignant pleural mesothelioma		*P* value
	No. of patients	%	No. of patients	%	
Total patients	30	100	79	100	
Gender					
Female	2	6.7	16	20.3	0.15
Male	28	93.3	63	79.7	
Age, years					
Median	71		67		
Mean ± standard error	69 ± 2		68 ± 1		0.53
Range	41–82		50–87		
ECOG PS					
0–1	27	90	56	71	0.04
2–4	3	10	23	29	
Side of disease					
Left	11	37	32	41	0.83
Right	19	63.	47	60	
Smoking habit					
Never	4	13	20	25	0.21
Smoker	26	87	59	75	
Pack years of smokers					
Median	55		50		
Mean ± standard error	60 ± 8		53 ± 5		0.45
Asbestos exposure					
No or unknown	4	13	7	9	
Yes	26	87	72	91	0.49

labeled with the anti-CD34 antibody were counted under light microscopy with a 200-fold magnification. The average counts were recorded as MVD for each patient.

Statistics

Counts were compared by the chi-square test. Continuous data were compared using the *t* test if the distribution of samples was normal, or using nonparametric tests (Mann-Whitney *U* test for comparison between two groups and Kruskal-Wallis test for comparison among three or more groups) if the sample distribution was asymmetrical. A nonparametric correlation method (Spearman test) was used to evaluate a correlation between CEC count and MVD.

Diagnostic performance of CEC was assessed by constructing a receiver operating characteristic (ROC) curve and was evaluated by calculating the area under each ROC curve (AUC–ROC). An AUC–ROC equal 1 denotes perfect discrimination of a test, while an AUC–ROC equal to 0.5 denotes complete lack of discrimination of a test. *P* value was calculated for the difference between each AUC–ROC and 0.5 (complete useless test).

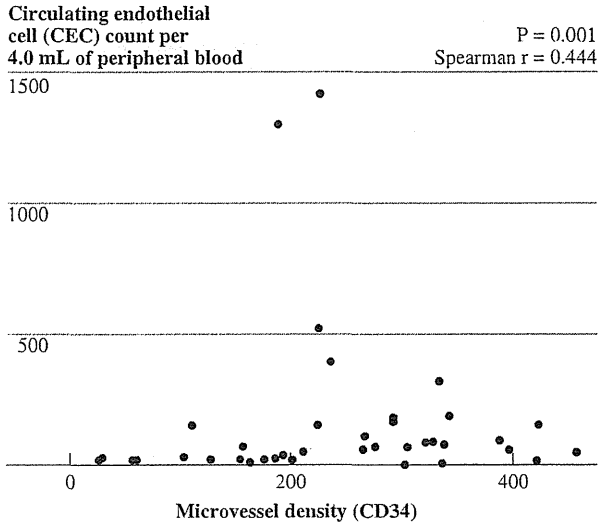

FIG. 1 Correlation between circulating endothelial cell (CEC) count and microvessel density (MVD)

Survival curves were generated using the Kaplan–Meier method, and the differences were assessed by the log-rank test. Cox's regression model was used for a multivariate analysis of prognostic factors.

For each test, 2-sided *P* values less than 0.05 were considered statistically significant. All statistical manipulations were performed using the SPSS for Windows software system (SPSS Inc., Chicago, IL).

RESULTS

Patient Characteristics

From September 2007 through November 2009, 110 consecutive patients were enrolled in the study. Pleural biopsy was performed, and final pathological diagnosis was established in all patients; one patient was excluded because biopsy specimen revealed pleural disseminated adenocarcinoma of the lung. Of 109 eligible patients, 30 were finally diagnosed pathologically with nonmalignant pleural diseases, and the other 79 were with MPM. Most patients had a history of asbestos exposure (Table 1).

Correlation Between CEC Count and MVD

First, we assessed a correlation between CEC count and MVD to examine whether CEC count in the peripheral blood can represent and can be a surrogate of tumor angiogenesis in MPM. MVD can be evaluated in 38 MPM

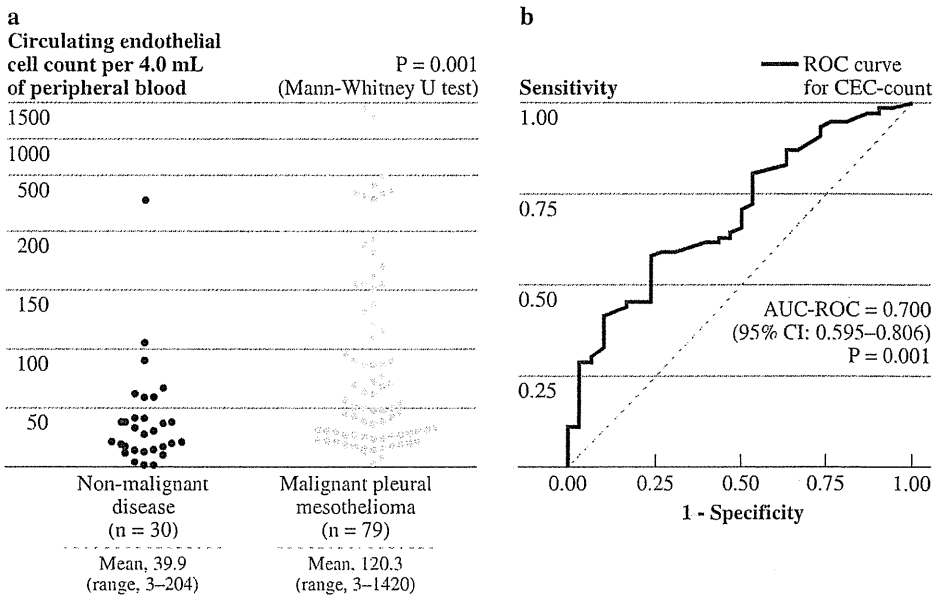

FIG. 2 Distribution of circulating endothelial cell (CEC) count in patients with nonmalignant diseases and in patients with malignant pleural mesothelioma. Receiver operating characteristic (ROC) curves for CEC count to discriminate malignant pleural mesothelioma from nonmalignant diseases. Area under each ROC curve (AUC–ROC) is calculated, and *P* value for testing the significance of difference from 0.5 (lack of discrimination) is indicated

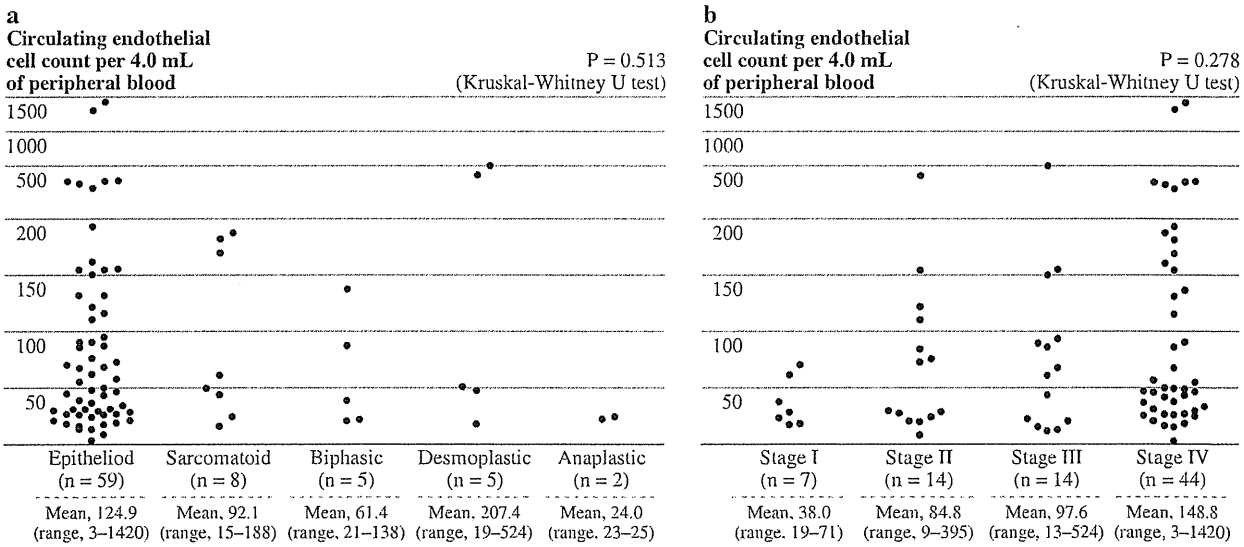

FIG. 3 Distribution of circulating endothelial cell (CEC) count in patients with malignant pleural mesothelioma according to histological subtype. Distribution of circulating endothelial cell (CEC) count in patients with malignant pleural mesothelioma according to clinical stage

patients. A significant positive correlation between CEC count and MVD was observed (correlation coefficiency [*r*], 0.444; $P = 0.001$) (Fig. 1).

CEC Count in MPM Patients and Nonmalignant Patients

Distributions of CEC count in nonmalignant patients and in MPM patients are shown in Fig. 2a, and CECs were significantly increased in MPM patients. The AUC–ROC for CEC in discrimination between MPM and nonmalignant diseases was 0.700 (95 % confidence interval [95 % CI], 0.595–0.806; $P = 0.001$) (Fig. 2b). According to the ROC analysis, the optimal cutoff value of CEC count was estimated to be "50 (cells/4.0 mL)" with the sensitivity and specificity of 49.4 and 76.7 %, respectively; the positive predictive value (PPV) and negative predictive value (NPV) were 84.8 and 36.5 %, respectively.

CEC Count in MPM Patients

Among MPM patients, there was no significant difference in CEC count according to histologic subtype (Fig. 3a) or clinical stage (Fig. 3b), whereas CECs might be increased in

TABLE 2 Univariate analysis of prognostic factors of patients with malignant pleural mesothelioma

	No. of patients	Overall survival (months)			HR		
		Median	95 % CI	*P* value	HR	95 % CI	*P* value
Gender				0.90			
Female	16	20	8–31		1		
Male	63	14	7–21		1.04	0.55–1.99	0.90
Age				0.29			
Lower (≤67 years)	42	19	12–26		1		
Higher (>67 years)	37	12	5–19		1.34	0.78–2.29	0.30
ECOG PS				<0.01			
0–1	56	19	16–22		1		
2–4	23	5	4–5		3.09	1.72–5.54	<0.01
Side of disease				0.46			
Left	32	13	5–21		1		
Right	47	15	9–21		1.23	0.71–2.13	0.46
Smoking habit				0.85			
Never	20	18	10–25		1		
Smoker	59	14	9–19		0.94	0.51–1.74	0.85
Asbestos exposure				0.52			
No or unknown	7	12	7–18		1		
Yes	72	15	10–20		1.40	0.50–3.90	0.52
Histological subtype				0.02			
Epithelioid	59	18	15–23		1		
Nonepithelioid	20	7	3–10		2.10	1.14–3.87	0.02
Clinical stage				0.02[a]			
Stage I	7	20	7–33				
Stage II	14	24	9–39				
Stage III	14	18	16–20				
Stage I–III	35	19	13–25		1		
Stage IV	44	10	4–16		1.96	1.13–3.39	0.02
Chemotherapy				<0.01			
Not performed	13	3	2–4		1		
Performed	66	18	12–23		0.24	0.12–0.47	<0.01
Surgery (complete resection by EPP)				0.40			
Not performed	74	15	9–20		1		
Performed	5	23	2–44		0.61	0.19–1.96	0.41
CEC count				0.03			
Lower (≤50/4.0 mL)	40	20	16–24		1		
Higher (>50/4.0 mL)	39	11	8–15		1.84	1.06–3.21	0.03

[a] For I–III vs IV

c-stage IV patients compared with stage I–III patients (mean CEC count, 151.8 and 80.6, respectively; $P = 0.190$ by the Mann-Whitney *U* test).

Univariate analyses revealed that poor PS, nonepithelioid histology, stage IV disease, no chemotherapy, and higher CEC count (>50/4.0 mL) were significantly associated with a poor prognosis (Table 2; Fig. 4). A multivariate analysis demonstrated that higher CEC count (hazard ratio [HR] and 95 % CI, 2.24 [1.24–4.43]; $P < 0.01$) as well as poor PS (HR, 3.07 [1.78–5.29]; $P < 0.01$) and nonepithelioid histology (HR, 2.45 [1.15–5.20]; $P = 0.02$) were independent prognostic factors (see Appendix Table 3).

DISCUSSION

The present study is the first clinical study on CEC in MPM. First, we showed a significant positive correlation between CEC count and MVD, indicating that CEC count in the peripheral blood can be a surrogate of tumor angiogenesis.

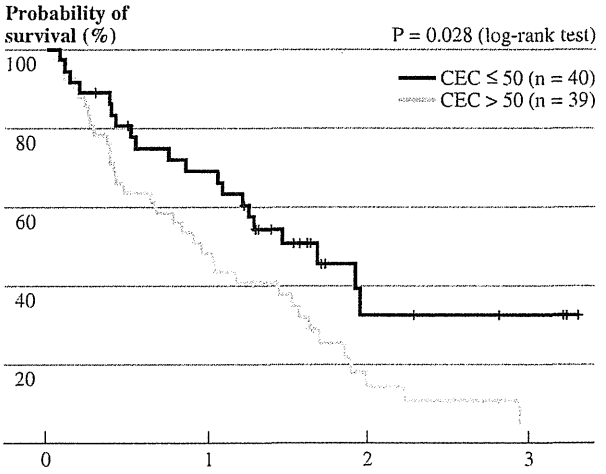

FIG. 4 Survival curves according to circulating endothelial cell (CEC) count

It is generally accepted that CECs are mature endothelial cells derived from damaged vascular wall, and CECs are increased in a variety of nonmalignant diseases such as sickle cell anemia, cytomegaro-virus infection, myocardial infarction, and endotoxinemia.[17,18] As reported in some experimental and clinical studies, CECs are also increased with development and progression of malignant tumors, but no previous study has been reported in MPM.[16–21] In contrast to CECs, circulating endothelial progenitor cells (CEPs) are thought to originate from bone marrow and to contribute to angiogenesis.[17,18] Thus, theoretically, CEP may be a more appropriate surrogate of tumor angiogenesis, but CEP might be inferior as a clinical marker because of no established assay to identify CEPs as well as an extremely low number of CEP identified in the peripheral blood of cancer patients.[17,18,23–25] Accordingly, we quantitatively evaluated CECs using the CellTrack system in the current study. The CellTrack system was originally developed to isolate circulating tumor cells (CTCs) with an antibody against the epithelial cell adhesion molecule (EpCAM), and the CTC assay has been approved as a clinical marker in monitoring blood from patients with metastatic breast, colorectal, and prostate cancer in the United States by the Food and Drug Administration (FDA).[26–28] The most important advantage of the CellTrack system is reproducibility, as the system is fully automated and is not operator dependent.[21] The CellTrack system can be used for isolation of CECs by using an anti-CD146 antibody, and some clinical studies documented that CEC count determined with the system was increased with tumor progression and was decreased in response to chemotherapy.[17–20] In the current study, we showed a positive correlation between CEC count and MVD, demonstrating that CECs might reflect tumor angiogenesis in MPM. Considering the biological nature and role of CECs, it can be speculated that CECs are increased with development and progression of tumor as a result of extended vascular damage and remodeling due to aggressive tumor angiogenesis and growth, and CEC can be an indirect surrogate of tumor angiogenesis and progression.[16–18] The present study demonstrated a significant, but not strong, correlation between CEC count and MVD (correlation coefficiency, 0.444), suggesting that a MVD measured with only one antibody against CD34 in a small biopsy specimen sometimes fails to represents angiogenesis of an entire tumor because of tumor tissue heterogeneity as well as difficulty in standardizing the measurement, particularly when evaluated with only one CD34 marker. In addition, a number of angiogenic factors and these receptors, such as vascular endothelial growth factor (VEGF) and VEGF-receptors 1, 2, and 3, can contribute to tumor angiogenesis. Thus, correlation between CEC count and MVDs evaluated with multiple markers such as CD31 as well as several angiogenic factor levels in the blood such as serum VEGF and soluble VEGFR-1 should be examined in future studies.

Next, we showed that CEC count was significantly higher in MPM patients than in nonmalignant patients, which was consistent with previous results documented in other malignant tumors.[16–18,21] In the present study, the ROC analysis showed a significant diagnostic performance of CEC in discrimination between MPM and nonmalignant diseases (ROC–AUC, 0.700; $P < 0.001$). Such findings may provide a new insight in the diagnosis of MPM, as only a few modalities are currently available in clinical practice.[5] Thus, CEC can be a useful diagnostic marker, which is noninvasively and repeatedly performed, to select patients who should proceed to invasive procedures such as VATS biopsy for establishment of pathological diagnosis. Nevertheless, at the cutoff of "50 (cells/4.0 mL)," the sensitivity of the CEC test was only 49.4 %, whereas the specificity was as high as 76.7 %. Thus, the CEC test alone is not enough for the diagnosis, and a combination of other markers such as SMRP and PET finding may provide more accurate diagnostic performance. Alternatively, when a lower cutoff value, "25 (cells/4.0 mL)," was used for the CEC test, the sensitivity rose to 77.2 %, whereas the specificity fell to 46.7 %. The cutoff value of "25" may be more appropriate in mass screening of high-risk population with apparent history of asbestos exposure. Previous studies demonstrating CEC count in healthy volunteers (mean, 32.6 and 38, respectively) may support the use of a lower cutoff value of 25 to increase the sensitivity.[20,21]

We failed to show a significant increase in CEC count along with advance in c-stage, whereas previous experimental and clinical studies showed that the CEC count reflects tumor volume in some solid tumors.[16–18] On the other hand, we demonstrated that a higher CEC count was a significant and independent factor to predict a poor prognosis in MPM. We failed to demonstrate a significant

prognostic value of c-stage, which was established as a strong prognostic factor in many other malignant tumors. In MPM, a prospective study conducted by the European Organization for Research and Treatment (EORTC) also revealed that c-stage was not a significant prognostic factor, and the EORTC prognostic model is now widely accepted and used in clinical practice.[4,29,30] Their results not only indicate limitation of conventional imaging in evaluation of c-stage in MPM, but also suggest that the current TNM system does not correctly represent extent of tumor progression. To establish the prognostic significance of CEC, future validation studies are warranted.

In conclusion, CEC was a promising noninvasive diagnostic marker in discrimination between MPM and nonmalignant diseases. In addition, CEC count, reflecting tumor angiogenesis, was a significant prognostic factor in MPM. Future validation studies should be conducted to establish its clinical value.

ACKNOWLEDGMENT This study was supported by The Special Coordination Funds for Promoting Science and Technology from the Japanese Ministry of Education, Culture, Sports, Science, and Technology, Grants-in-Aid for Scientific Research (KAKENHI B 24390335) from the Japan Society for the Promotion of Science (JSPS), and UOEH Grant for Advanced Research (H24-1) from University of Occupational and Educational Health.

CONFLICT OF INTEREST None declared.

APPENDIX

See Figs. 5, 6 and Table 3

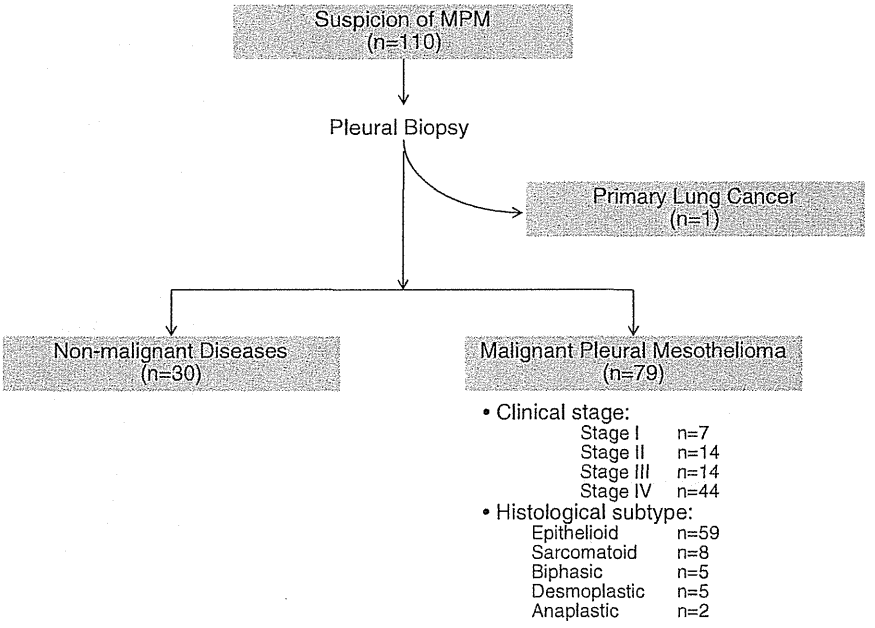

FIG. 5 Flowchart of diagnosis of patients enrolled in the study

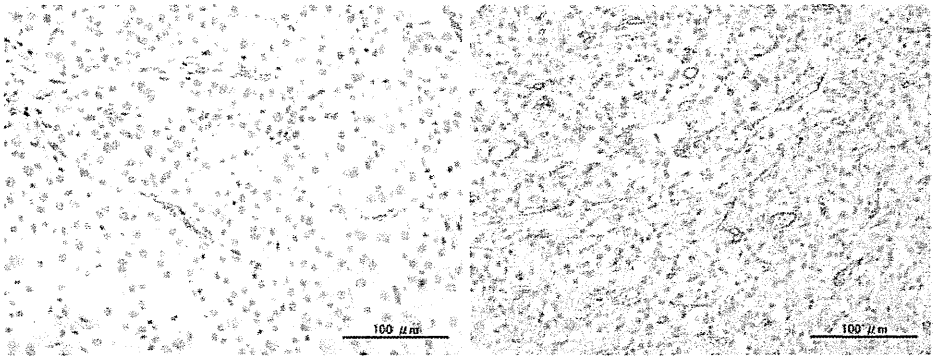

Epithelioid-type MPM with a lower MVD (29) and a lower circulating endothelial cell (CEC) count (27)

Epithelioid-type MPM with a higher MVD (388) and a higher circulating endothelial cell (CEC) count (73)

FIG. 6 Immunohistochemical staining with an anti-CD34 antibody in malignant pleural mesothelioma (MPM) to evaluate intratumoral microvessel density (MVD)

TABLE 3 Multivariate analysis of prognostic factors of patients with malignant pleural mesothelioma

	HR	95 % CI	*P* value
Gender			
Female	1		
Male	1.67	0.40–6.94	0.48
Age			
Lower (≤67 years)	1		
Higher (>67 years)	0.97	0.51–1.86	0.93
ECOG PS			
0–1	1		
2–4	3.07	1.78–5.29	<0.01
Side of disease			
Left	1		
Right	2.08	0.98–4.26	0.05
Smoking habit			
Never	1		
Smoker	0.68	0.25–1.82	0.44
Asbestos exposure			
No or unknown	1		
Yes	0.52	0.16–1.63	0.26
Histological subtype			
Epithelioid	1		
Nonepithelioid	2.45	1.15–5.20	0.02
Clinical stage			
Stage I–III	1		
Stage IV	1.06	0.77–1.46	0.73
Chemotherapy			
No	1		
Yes	0.40	0.16–1.01	0.05
Surgery (complete resection by EPP)			
No	1		
Yes	1.14	0.32–4.04	0.84
CEC count			
Lower (≤50/4.0 mL)	1		
Higher (>50 /4.0 mL)	2.24	1.24–4.43	<0.01

REFERENCES

1. Ismail-Khan R, Robinson LA, Williams CC, Garrett CR, Bepler G, Siomn G. Malignant pleural mesothelioma: a comprehensive review. *Cancer Control.* 2006;13:255–63.
2. Tsiouris A, Walesby RK. Malignant pleural mesothelioma: current concept in treatment. *Nat Clin Practice Oncol.* 2007;4:3 44–52.
3. Scherpereel A, Astoul P, Baas P, Berghmans T, Clayson H, de Vuyst P, et al. Guidelines of the European Respiratory Society and the European Society of Thoracic Surgeons for the management of malignant pleural mesothelioma. *Eur Respir J.* 2010;35:479–95.
4. Stahel RA, Weder W, Lievens Y, Felip E. Malignant pleural mesothelioma: ESMO clinical practice guidelines for diagnosis, treatment and follow-up. *Ann Oncol.* 2010;21:v126–8.
5. van der Bij S, Schaake E, Koffijberg H, Burgers JA, de Mol BAJM, Moons KGM. Markers for the non-invasive diagnosis of mesothelioma: a systematic review. *Br J Cancer.* 2011;104:1325–33.
6. Lee AY, Raz DJ, He B, Jablons DM. Update on the molecular biology of malignant pleural mesothelioma. *Cancer.* 2007;109: 1454–61.
7. Sculier JP, Berghmans T, Meert AP. Update in lung cancer and mesothelioma. *Am J Respir Crit Care Med.* 2010;181:773–81.
8. Cao CQ, Yan TD, Bannon PG, McCaughan BC. A systemic review of extrapleural pneumonectomy for malignant pleural mesothelioma. *J Thorac Oncol.* 2010;5:1692–703.
9. Vogelzang NJ, Rusthoven JJ, Symanowski J, Denham C, Kaukel E, Ruffie P, et al. Phase III study of pemetrexed in combination with cisplatin versus cisplatin alone in patients with malignant pleural mesothelioma. *J Clin Oncol.* 2003;21:2636–44.
10. Ray M, Kindler HL. Malignant pleural mesothelioma: an update on biomarkers and treatment. *Chest.* 2009;136:888–96.
11. Folkman J. Anti-angiogenesis: new concept for therapy of solid tumors. *Ann Surg.* 1972;175:409–16.
12. Yano S, Li Q, Wang W, Yamada T, Takeuchi S, Nakataki E, et al. Antiangiogenic therapies for malignant pleural mesothelioma. *Front Biosci.* 2011;16:740–8.
13. Ohta Y, Shridhar Y, Bright RK, Kalemkerian GP, Du W, Carbone M, et al. VEGF and VEGF type C play an important role in angiogenesis and lymphangiogenesis in human malignant mesothelioma tumours. *Br J Cancer.* 1999;81:54–61.
14. Kumar-Singh S, Weyler J, Martin MJ, Vermeulen PB, E. van Marck. Angiogenic cytokines in mesothelioma: a study of VEGF, FGF-1 and -2, and TGF beta expression. *J Pathol.* 1999;189: 72–8.
15. Tolnay E, Kuhnen C, Wiethege T, König JE, Voss B, Müller KM. Hepatocyte growth factor/scatter factor and its receptor c-Met are overexpressed and associated with an increased microvessel density in malignant pleural mesothelioma. *J Cancer Res Clin Oncol.* 1998;124:291–6.
16. Monestiroli S, Mancuso P, Burlini A, Pruneri G, Dell'Agnola C, Gobbi A, et al. Kinetics and viability of circulating endothelial cells as surrogate of angiogenesis marker in an animal model of human lymphoma. *Cancer Res.* 2001;61:4341–4.
17. Mancuso P, Rabascio C, Bertolini. Strategies to investigate circulating endothelial cells in cancer. *Pathophysiol Haemost Thromb.* 2004;33:503–6.
18. Strijbos MH, Gratama JW, Kraan J, Lamers CH, den Bakker, Sleijfer S. Circulating endothelial cells in oncology: pitfalls and promises. *Br J Cancer.* 2008;98:1731–5.
19. Beerepoot LV, Mehra N, Vermaat JSP, Zonnenberg BA, Gebbink MFGB, Voest EE. Increased levels of viable circulating endothelial cells are an indicator of progressive disease in cancer patients. *Ann Oncol.* 2004;15:139–45.
20. Kawaishi M, Fujiwara Y, Fukui T, et al. Circulating endothelial cells in non-small cell lung cancer patients treated with carboplatin and paclitaxel. *J Thorac Oncol.* 2009; 4:208-13.
21. Rowand JL, Martin G, Doyle GV, Miller MC, Pierce MS, Connelly MC, et al. Endothelial cells in peripheral blood of healthy subjects and patients with metastatic carcinomas. *Cytometry Part A.* 2007;71A:105–13.
22. Rusch VW. A proposed new international TNM staging system for malignant pleural mesothelioma from the international mesothelioma interest group. *Lung Cancer.* 1996;14:1–12.
23. Lyden D, Hattori K, Dias S, Costa C, Blaikie P, Butros L, et al. Impaired recruitment of bone-marrow-derived endothelial and hematopoietic precursor cells blocks tumor angiogenesis and growth. *Nat Med.* 2001;7:1194–201.
24. Peters BA, Diaz LA, Polyak K, Meszler L, Romans K, Guinan EC, et al. Contribution of bone-marrow-derived endothelial cells to human tumor vasculature. *Nat Med.* 2005;11:261–2.